UNIVERSITY of the
WESTERN CAPE

Investigation of the anti-obesity effects of citrate-capped gold nanoparticles on 3T3-L1 cells and their genetic profiling

Anelisiwe Mbengashe

Student Number: 3265578

A mini thesis submitted in partial fulfillment of the requirements for the degree Magister Scientiae in Nanoscience Department of Biotechnology, University of the Western Cape

Supervisor: Dr. Nicole Remaliah Samantha Sibuyi

Co-supervisor: Dr. Jyoti Rajan Sharma

March 2023

saMRC advancinglife

DECLARATION

I **Anelisiwe Mbengashe** declare that "**Investigation of the anti-obesity effects of citrate-capped gold nanoparticles on 3T3-L1 cells and their genetic profiling**" submitted for an MSc degree at the University of the Western Cape is my own work and has not been previously submitted for a degree at this or any other university, and that all sources used, cited, or quoted have been acknowledged and referenced accordingly.

Anelisiwe Mbengashe

Student number: 3265578

Signature: **Date: March 2023**

ABSTRACT

The incidence and prevalence of obesity and its related diseases has nearly tripled and is increasing at an alarming rate worldwide. Several modern methods for the management and treatment of obesity are available, with anti-obesity drugs being the preferred choice. Despite the availability of anti-obesity drugs, their therapeutic capabilities are hampered by drug toxicity and undesirable side effects, implying the need for alternative therapies. Thus, nanotechnology-based strategies may provide a novel beneficial mediator in the management and treatment of obesity.

Gold nanoparticles (AuNPs) have drawn much attention in various biomedical applications due to their unique physicochemical properties, offering significant advances for the development of targeted therapeutics with sustainable effects. In a previous study, we have shown that exposure of 14 nm citrate-capped AuNPs (cAuNPs) to human colorectal adenocarcinoma (Caco-2) cells downregulated genes involved in lipid metabolism. This suggested that 14 nm cAuNPs have a promising future in the treatment of obesity and obesity-related disorders; and can overcome some of the limitations associated with anti-obesity treatments. Therefore, the current study investigated the anti-obesity and molecular effects of 14nm cAuNPs in 3T3-L1 differentiated adipocytes.

The 14 nm cAuNPs were synthesized using the Turkevich/citrate reduction method, where tri-sodium citrate was used in the reduction of hydrogen tetrachloroaurate ($HAuCl_4.3H_2O$). The formation of cAuNPs was monitored by colour changes and was later characterized by Ultraviolet-visible spectroscopy (UV-Vis), dynamic light scattering (DLS) and High-Resolution Transmission Electron Microscope (HR-TEM). The concentration of the resulting cAuNPs was evaluated by Inductively Coupled Plasma Atomic Optical Emission Spectroscopy (ICP-OES). The stability of the cAuNPs in various buffers was evaluated by monitoring

changes in the UV-Vis spectra over an incubation period of 0 - 96 h, at 37°C and/or room temperature (RT). The 3T3-L1 preadipocytes were stimulated and differentiated into 3T3-L1 adipocytes with cocktail media (1 µg/mL insulin, 0.5 mM isobutylmethyl xanthine (IBMX), and 1 µM dexamethasone (DEX)). The undifferentiated and differentiated 3T3-L1 cells were treated with various concentrations of cAuNPs for 24 – 72 h. Cytotoxic and anti-obesity effects of the cAuNPs on were confirmed using the Water Soluble Tetrazolium (WST)-1 cell viability assay and Oil Red O (ORO) staining, respectively. The effect of cAuNPs on 86 genes involved in the adipogenesis pathway was investigated on differentiated 3T3-L1 cells by the Mouse Adipogenesis RT² PCR Array and measured by real-time quantitative polymerase chain reaction (RT-qPCR).

The 14 nm cAuNPs with an absorption peak of 521 nm and zeta potential of -27.8 mV were successfully synthesized using the citrate reduction method. HR-TEM confirmed the cAuNPs to be relatively spherical and monodispersed with a core diameter of 14 nm. The cAuNPs at concentrations up to 400 nM were nontoxic to both the undifferentiated and differentiated 3T3-L1 cells. Treatment of the 3T3-L1 adipocytes with cAuNPs was shown to quantitatively reduce lipid content. In addition, the PCR array revealed 35 differentially expressed genes (DEGs), five DEGs (*Dlk1, Klf2, Runx1t1, Rxra, VDR*) were significantly downregulated in differentiated 3T3-L1 cells. The findings in this study indicated that cAuNPs have the potential to exert anti-obesity properties. However, further research into the *in vivo* effects and the molecular mechanism of cAuNPs in obesity models is required.

KEYWORDS

3T3-L1 cells

Adipocytes

Gold nanoparticles

Obesity

Nanotechnology

ACKNOWLEDGEMENTS

First and foremost, I would like to thank the **Lord Almighty** for providing me with the opportunity, guidance, strength, and mental power to succeed in this part and all of my academic endeavors.

I wish to express my heartful thanks to my supervisor, **Dr. Nicole Sibuyi**, for her valuable knowledge, keen interest, and constant encouragement. Her guidance helped me in all the time of research and writing of this thesis. Even though most times ignoring her calls would be an option, somehow, I felt motivated and encouraged every time I spoke to her. I could not have imagined having a better advisor and mentor.

I am equally grateful to my co-supervisor, **Dr Jyoti Sharma**, for her assistance, persistence, patience, and support. Thank you for taking the time to thoroughly train and be with me in this "adventurous" gene expression journey.

I would like to show my appreciation to **Prof. Mervin Meyer** and **Prof. Abram Madiehe** for allowing me to use the lab and for providing resources to carry out my research; for listening to all my "complaints", being there for guidance, and providing mentorship and constructive comments towards my development as a researcher.

I would like to thank all the people I've met during my journey: **colleagues**, **lab mates** and those I can sincerely call **friends**. It is their kind help and support that have made my study and life in the lab and outside a wonderful time. The games, "library", outings, and everything else in between made it worthwhile. I have had the great pleasure of working with my mentor, Mr. **Thendo Mabuda**. I sincerely wish you all the best on the completion of your PhD.

I would like to extend my gratitude to the DSI National Nanoscience Post Graduate Teaching and Training Platform (**NNPTTP**) – with special thanks extended to Mrs. Valencia Jamalie;

the DST/Mintek Nanotechnology Innovation Centre (**NIC**), and the South African Medical Research Council (**SAMRC**), whom without this research would not have been possible.

Last but not least, to my beloved family, the **Mbengashes** and **Hyeras**, thank you. Sincere gratitude for their never-ending support, encouragement, and prayers. I love you all. My appreciation also goes to my sister **Nobotho Mbengashe**, thank you for always believing in me. My husband, **Allan Hyera**, for your tremendous understanding in my absence, patience, support and motivation. I love you mpenzi wangu – you are my rock.

PRESENTATIONS

Mbengashe, **A**., Sharma, J., Meyer, S., Fadaka A. O., Wusu, D. A., Meyer, M., Madiehe, A. M., Sibuyi, N. R. S. The 11th International Conference of the African Materials Research Society (AMRS2022). Dakar, Senegal. 12-15 December 2022. [Oral Presentation]. **Awarded**: ACS Best Oral Presentation Award

Mbengashe, **A**., Sharma, J., Meyer, S., Fadaka A. O., Wusu, D. A., Meyer, M., Madiehe, A. M., Sibuyi, N. R. S. Investigation of the cytotoxic and anti-obesity effects of citrate-capped gold nanoparticles on 3T3-L1 cells. The 8th International Conference on Nanoscience and Nanotechnology in Africa (NanoAfrica 2022). Cape Town, South Africa. 26-28 October 2022. [Oral Presentation]

PUBLICATION

Sibuyi, N. R. S., **Mbengashe A**., Nqakala, Z. B., Ajmal, A. A., Mgijima, T., Mashilo, C. M., Matshaya, A., Seele, P., Meyer, S., Meyer, M., Onani, M. O., Madiehe, A. M., Fadaka, A. O. (2023). Chapter 13 Carbon dots in drug delivery. In Carbon Dots in Biology, Berdimurodov, E.T., Verma, D.K., Eds.; De Gruyter: Berlin, Boston, 2023; pp. 283-312. https://doi.org/10.1515/9783110799958-013

TABLE OF CONTENTS

LIST OF FIGURES

LIST OF TABLES

CHAPTER 1: LITERATURE REVIEW

1.1 Introduction

Obesity prevalence has risen dramatically since the 1980s. This global occurrence is of grave concern, imposing an additional burden on developing countries such as India and Brazil, and spreading even to Sub-Saharan African regions, all of which have a significant impact on the global economy (Mercer et al., 2019). According to the World Health Organization (WHO) global statistics, more than 1.9 billion adults (18 years and older) were overweight, with over 650 million being obese (WHO, 2020). Furthermore, more than 41 million children under the age of five were estimated to be overweight or obese (WHO, 2020).

Obesity is also a risk factor for the development of other chronic diseases with high morbidity and mortality (Cesare et al., 2019) such as type 2 diabetes (T2D) (Kawasaki et al., 2018), cardiovascular diseases (CVDs) (Kumar, 2019; Umer et al., 2017), hypertension (Kumar, 2019), dyslipidemia (Kawasaki et al., 2018), and some types of cancers (Hidayat et al., 2018). Given the severity of obesity, the health expenditures generated by obesity and its comorbidities are significant. Obesity and its associated health complications have staggering costs, not only in terms of healthcare expenditure but also in terms of quality of life, highlighting the importance of implementing prevention strategies (Mercer et al., 2019).

Obesity as a chronic disease is currently managed primarily through lifestyle modification, surgery (Smith et al., 2020) and pharmacotherapy. The pharmacological strategies are used to manage obesity through various mechanisms such as satiety/appetite suppression, reduction of fat absorption or increment of fat metabolism (Tak & Lee, 2021). However, drug use is associated with significant and intolerable side effects, which has resulted in the withdrawal of

several anti-obesity drugs from the market (Bays et al., 2022). As a result, safer alternatives that are effective and have few or no side effects are needed.

Recent studies have focused on the development of innovative therapeutic agents as alternative medicine. Nanomedicine is a fast-growing branch of nanotechnology that has great promise in disease treatment. By taking advantage of the small size and large surface area of nanoparticles (NPs), nanotechnology seeks to design and develop nanomedicines that are cost-effective and have high efficacy, while inducing the lowest possible side effects (Iravani, 2011). Metallic nanoparticles, especially from noble metal (gold), have been developed and reported to have interesting medical applications. The biomedical application of AuNPs is being extensively researched due to their high biocompatibility, ease of preparation, catalytic, and redox properties (Shittu et al., 2017). Experimental studies have identified critical therapeutic actions of AuNPs in various diseases such as anti-cancer, antidiabetic, antimicrobial, anti-inflammatory, and antioxidant effects (Sekar et al., 2022). However, the health hazards or potential risks associated with exposure to AuNPs is largely unknown. The challenge of nanomaterial-based studies is to evaluate, in a consistent way, the mechanism of action and their associated toxicity since it might not be immediate.

Analyzing gene expression is a logical way to study the precise mechanisms of NP toxicity. In this view, recent studies have also shown that NPs can change gene expression and potentially alter cellular functions (Sousa De Almeida et al., 2021). Thus, understanding the molecular mechanism of NPs on obesity pathways can provide guidance for the treatment of obesity and obesity-related metabolic diseases.

1.2 Obesity

Obesity is caused by an abnormal accumulation of excess energy within the adipose tissues (ATs) resulting from a chronic imbalance between energy intake and energy expenditure (Gregg & Shaw, 2017). Obesity pathogenesis is extremely complex, and it is widely recognized that genetic (congenital) and environmental factors both play a key role in its development. Poor dietary habits, and sedentary lifestyles, are major environmental factors that contribute to the development and progression of obesity (Yadav & Jawahar, 2022).

Obesity is mostly measured based on the Body Mass Index (BMI) (WHO, 2020) which is calculated by dividing the bodyweight in kilograms by the square of the height in meters (kg/m^2) to categorize adults as either underweight, healthy, overweight, or obese (Table 1.1). A BMI greater than or equal to 25 kg/m^2 is considered overweight, and a BMI greater than or equal to 30 kg/m^2 is considered obese (WHO, 2020). Although BMI is widely used, it should be noted that the waist-to-hip circumference ratio (WHR) (normally less than 0.95 in men and 0.85 in women) is also a valuable prognostic indicator for obesity than BMI (Pike & Grosse, 2018).

Table 1.1: BMI classification of bodyweight (WHO, 2020)

Classification	**BMI (kg/m^2)**	**Description**
Underweight	< 18.5	Thin
Normal weight	18.5 - 24.9	Healthy, Normal, acceptable
Grade 1 overweight	25.0 - 29.9	Overweight
Grade 2 overweight	30.0 - 39.9	Obesity
Grade 3 overweight	≥ 40.0	Morbid obesity

This is because, WHR, as compared to BMI, considers body fat distribution, distinguishes between fat and muscle mass. WHR provides a more accurate estimate of health risk as body composition changes with age. In addition to the WHR, waist circumference is also used in obesity research. Both measures are related to abdominal or visceral obesity, i.e., body fat stored around the stomach and abdomen, while the skinfold thickness test quantifies the subcutaneous fat which is located just beneath the skin.

Furthermore, computed tomography or magnetic resonance imaging are available to quantify central fat mass and visceral fat, but these methods are expensive and time-consuming and therefore unsuitable for routine clinical screening (WHO, 2008).

1.3 Prevalence of obesity

Obesity, which was mostly prevalent in developed countries, has recently become a major life-threatening disease in both developed and developing countries, with the prevalence of overweight and obesity increasing in countries where hunger is still prevalent (Mercer et al., 2019). According to recent statistics, at least 2.8 million people die each year as a result of complications related to overweight or obesity (WHO, 2020). The prevalence of obesity had nearly tripled from 1975 to 2016, worldwide. According to the 2016 WHO statistics, estimates show that overweight affected approximately 1.9 billion adults, with obesity affecting approximately 650 million adults. This equates to 39% of adults aged 18 and above being overweight (Figure 1.1(a)), with 13% being obese (Figure 1.1b) (WHO, 2022). The rapid increase in the number of children under the age of five who are overweight or obese is also a cause for concern, with over 41 million children worldwide either overweight or obese. This is a contributing factor to an increase in childhood T2D rates, which was previously thought to be a disease that only affected adults. The current estimates indicate that more than half of the

world's population will be overweight or obese by 2030 (Kelly et al., 2008), further escalating the seriousness of the disease as a major risk factor for debilitating diseases such as heart disease, high blood pressure, respiratory complications, arthritis and some types of cancers (colon, rectum, prostate, ovaries, endometrium, breast, and gallbladder) (Fruh, 2017). In the midst of a serious health crisis caused by the severe acute respiratory syndrome coronavirus 2 (SARS-CoV-2) pandemic, emerging data show that obesity fueled the Corona virus (COVID-19) infections and worsened disease course and prognosis, leading to higher mortality rates. Thus, the lockdown that took place due to COVID-19 pandemic has altered lifestyle habits and fostered an obesogenic environment, which has also amplified the obesity pandemic, with long-term implications for the prevalence of overweight and obesity (Manca et al., 2022).

1.4 Prevalence of obesity in South Africa

South Africa, a middle-income country at Africa's southernmost tip, has one of the highest rates of overweight and obese people compared to other African countries and the world at large (Figure 1.1). Approximately 69% of South African women are overweight, with 42% being obese. These figures are higher than those reported for women in the United States of America (USA), a country known for its high rates of overweight and obesity, which is at 62% overweight and 34% obese (Toriola et al., 2016). Worryingly, many of these women are of child-bearing age and potential candidates for abnormal intrauterine programming, increasing the risk of their offspring developing obesity and metabolic disease later in life (O'hara et al., 2021).

Furthermore, obesity increases the risk of noncommunicable diseases, and in SA, it is estimated that being overweight is responsible for up to 87% of T2D cases (Pheiffer et al., 2021). This places a significant burden on an already stressed healthcare system, which is already dealing

with high rates of human immunodeficiency virus/acquired immunodeficiency syndrome (HIV/AIDS) and tuberculosis. Without proper strategies to combat these rates, the WHO predicted that obesity-related chronic diseases will account for 60% of global deaths by 2025 (WHO, 2020). These projections highlight the critical need to address the obesity epidemic.

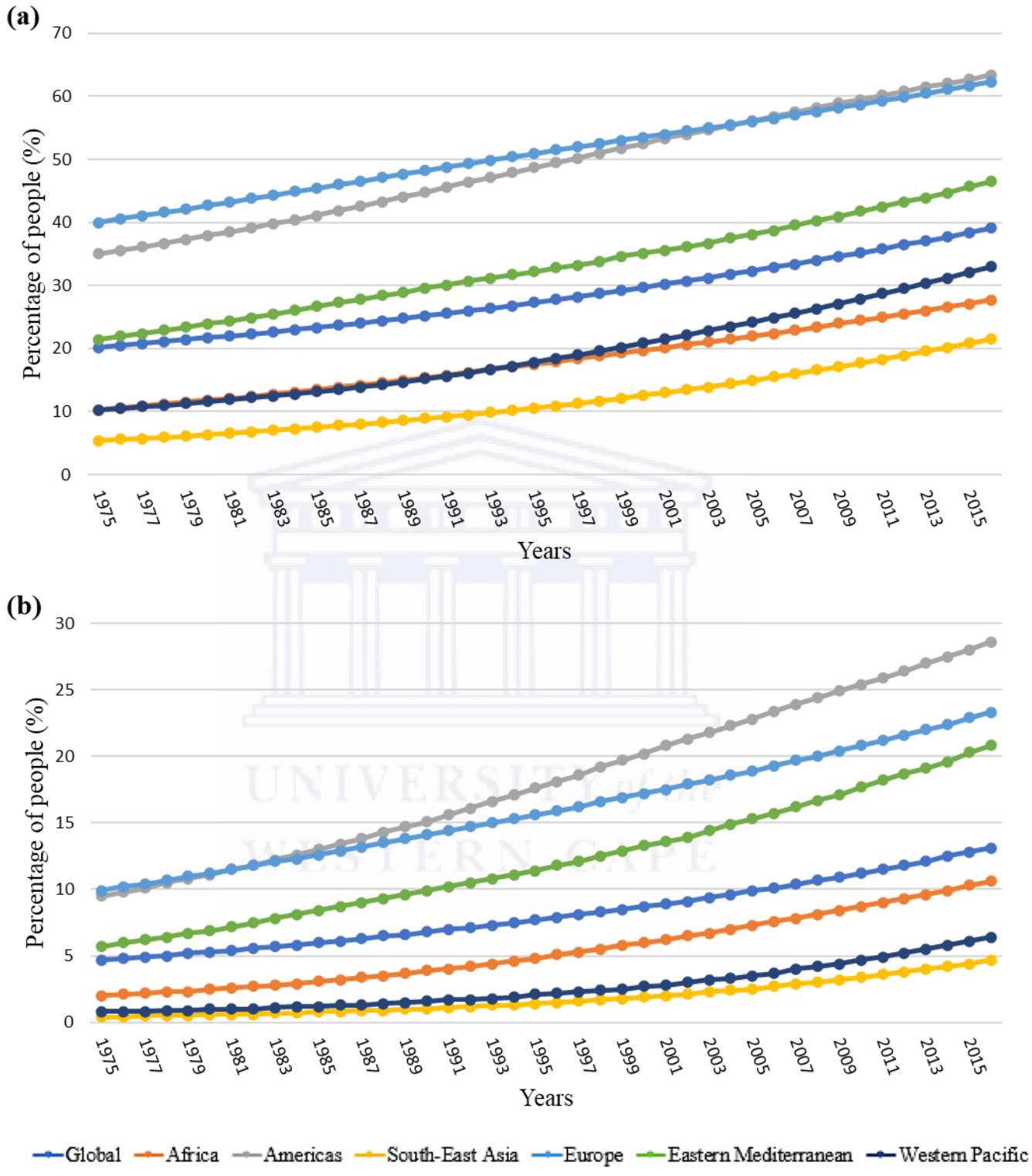

Figure 1.1: Prevalence of **(a)** overweight and **(b)** obesity among adults from 1975 to 2016 worldwide. Adapted from (WHO, 2022)

1.5 Role of ATs in the development of obesity

Adipose tissue (AT) is a type of specialized connective tissue found in all mammalian species, classified into two types: white adipose tissue (WAT) and brown adipose tissue (BAT). WAT is primarily used to store energy in the form of triglycerides (TGs). BAT, on the other hand, functions as a thermogenic organ, assisting in the dissipation of energy in the form of heat (Eckel, 2018). Subcutaneous and visceral AT are the two main WATs in the body, while interscapular and mediastinal are the main BATs. WAT is the most common type of adipose tissue in adults and the only tissue in the body that can change mass even after reaching adulthood. The stromal-vascular fraction of AT includes pre-adipocytes, fibroblasts, endothelial cells, macrophages, and adipocytes (Gavin, 2019).

In the early 1950s, AT was simply thought of as a metabolically inactive fat depot that serves as insulation and mechanical support for the organs (Eckel, 2018). However, AT was later linked to more fundamental functions and identified as a major energy regulation site. AT has two major functions: it stores excess energy as TGs, and it releases free fatty acids for energy production into the muscle and liver for fatty acid oxidation (Richard et al., 2020).

The importance of this tissue is further exemplified by the discovery of its secreted hormones known as adipokines, e.g. leptin discovered in 1994, added a new dimension to the understanding of AT function (Richard et al., 2020). This molecule, which can regulate food intake and energy expenditure, is secreted by adipocytes and its deficiency causes obesity. Subsequent research has revealed that adipocytes secrete a variety of other molecules that are involved in the regulation of various physiological functions. These studies led to the recognition of AT as an endocrine organ. Nonfat cells in AT are also known to secrete a variety of molecules. These secretory molecules play an important role in the regulation of whole-body homeostasis and metabolism. Any disruption in AT formation, lipoatrophy, or obesity causes

abnormal secretion of adipokines, resulting in a variety of metabolic complications such as insulin resistance, T2D, and CVD (Chait & den Hartigh, 2020). Further confirming that the interplay between genes expressed in AT and environmental factors contribute to the etiology of obesity.

1.6 Adipogenesis and molecular mechanism related to obesity

Obesity is characterized by AT expansion due to increased size (hypertrophy) or increased number (hyperplasia) of adipocytes. Adipocytes are the main cellular component of the AT, accounting for approximately 70% of the total volume. Since mature adipocytes cannot divide (Longo et al., 2019), adipocyte regeneration is dependent on the recruitment and terminal differentiation of pre-adipocytes or adipose-derived stem cells to form new adipocytes (adipogenesis). Adipogenesis is the process by which new adipocytes are formed by the differentiation of pre-adipocytes into mature adipocytes (Longo et al., 2019).

In vitro cell line models, such as 3T3-L1 cells, have aided in the understanding of the adipogenesis process. Pluripotent stem cells differentiate into mesenchymal precursor cells, which can differentiate into a variety of cell lineages such as pre-adipocytes, chondroblasts, osteoblasts, and myoblasts. Growth arrest, post-confluence mitosis, clonal expansion, early differentiation, and terminal differentiation are all stages involved in differentiation of pre-adipocytes into mature adipocytes (Eckel, 2018). The differentiation of these stem cells into adipocytes follows two distinct phases. In the first phase, pluripotent stem cell commits to adipocyte lineage and undergoes mitotic clonal expansion. In the second phase, the committed adipocyte precursors or preadipocytes differentiate into mature adipocytes by acquiring all the necessary machinery for lipid synthesis and transport, insulin sensitivity and secretion of adipose specific proteins (Ruiz-Ojeda et al., 2016; Todorčević et al., 2017). Adipogenesis is

accompanied by morphological changes following each stage of differentiation. Adipose stem cells commit to preadipocytes in response to adipogenic stimuli, which remain elusive *in vivo*. Preadipocytes during AT development change their shape from a fibroblast structure to round fat cells with characteristic lipid droplets shown in figure 1.2. Once committed, preadipocytes develop an adipocyte-specific gene expression pattern, as well as the formation of lipid droplets. Multilocular lipid droplets (LDs) eventually fuse to form a large, distinct LD that characterizes mature white adipocytes (Dufau et al., 2021).

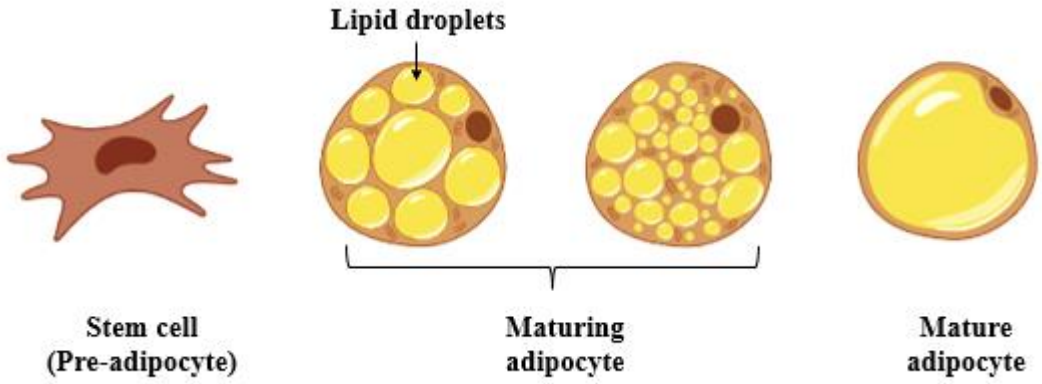

Figure 1.2: Schematic overview of adipogenesis adapted from Dufau *et al*. (Dufau et al., 2021).

It has been shown that during adipocyte differentiation, a transcriptional cascade is initiated by various signals emanating from both intracellular and extracellular environment culminating in the induction of various transcriptional factor genes. Peroxisome proliferator and activated receptor gamma (PPARγ) and cytosine-cytosine-adenosine-adenosine-thymidine (CCAAT)-enhancer-binding proteins (C/EBPα, β and δ) family of transcription factors, play a key role in the regulation of the transcriptional events occurring during adipocyte differentiation (Lee & Ge, 2014). The interplay of these gene products are involved in the formation of fully differentiated and functional adipocytes resulting in lipid accumulation and insulin sensitivity (Murphy et al., 2019).

1.7 The PPARs nuclear receptor

PPARs are classified into three isoforms: PPARα, PPARδ, and PPARγ. PPARγ is said to be the most adipogenic of these isoforms. Although PPARδ is widely expressed and has been shown to be adipogenic, its specific agonist did not promote adipogenesis in 3T3-L1 cells, whereas PPARγ agonist significantly enhanced adipogenesis (Audano et al., 2022). This demonstrates that PPARγ plays a major role in adipogenesis while PPARδ plays a minor role. PPARγ is essential for adipocyte differentiation. In the absence of PPARγ, ectopic expression of PPARγ in preadipocyte fibroblast cells induced adipocyte differentiation, and no single factor has been identified that accelerates or induces adipogenesis (MacDougald & Lane, 1995).

PPARγ expression or activation is caused by all signaling pathways involved in adipocyte differentiation. All of the known pro-adipogenic factors have been shown to work in part by activating PPARγ. PPARγ is highly expressed in adipocytes and exists in two isoforms, PPARγ 1 and 2, that are formed through alternative splicing. Both of these isoforms are involved in adipogenesis, but PPARγ 1 is also found in cell types other than adipocytes. Ectopic expression of PPAγR 1 and 2 in PPARγ -/- fibroblasts revealed that PPARγ 2 promotes adipocyte differentiation more efficiently than PPARγ 1 (Ahmad et al., 2020; Audano et al., 2022).

PPARγ expression is very low in 3T3-L1 preadipocytes, but it increases dramatically in differentiated adipocytes. When PPARγ is activated, it binds to DNA as a heterodimer with the retinoid X receptor (RXR) and activates the expression of numerous genes that regulate adipogenesis, lipid uptake, and lipid metabolism; gradually converting preadipocytes to adipocytes. Endogenous PPARγ ligands are fatty acids and their metabolites. Sterol regulatory element binding proteins-1c (SREBP-1c) and C/EBPβ have been shown to increase PPAR

ligand production (MacDougald & Lane, 1995). Many synthetic PPAR ligands have been identified, including thiazolidinediones (TZDs), a class of drugs used to increase insulin sensitivity. PPARγ ligands exert their effects by binding to the ligand binding domain (LBD). The PPARγ LBD contains 270 amino acid residues and is located at the receptor's C-terminus. Transactivation and dimerization regions are also found in LBD. The mechanism of PPARγ activation has been elucidated through biochemical and structural studies. Binding of ligand to LBD causes conformational rearrangement of the transcriptional activation function two (AF-2) region during activation. This causes corepressor proteins to be displaced and increases the recruitment of coactivators required for gene transcription (Capelli et al., 2016).

PPARγ is required not only for the induction of adipogenesis, but also for the maintenance of the adipocyte phenotype and function. Overexpression of dominant negative PPARγ in adipocytes resulted in TG accumulation and adipocyte dedifferentiation. PPARγ knockout in adipocytes resulted in adipocyte death and insulin resistance in the liver and AT (Ahmad et al., 2020). Although PPARγ alone has been shown to be sufficient for initiating the adipocyte transcriptional cascade and maintaining adipocytes, a synergistic effect with C/EBPα has been demonstrated. Ectopic expression of either of these genes has been shown to increase expression of the other, implying a mutual interaction for enhancing adipogenesis (Ritter et al., 2022).

1.7.1 CCAAT-enhancer-binding proteins (C/EBPs)

Members of the C/EBP family of transcription factors, C/EBPδ and C/EBPβ, play a temporal role in adipocyte differentiation. C/EBPα is the most important isoform for adipogenesis and has been shown to increase the expression of many adipogenic genes, including PPARγ. C/EBPδ, and C/EBPβ are known to induce C/EBPα expression by binding to its promoter

during the early stages of adipocyte differentiation. They are visible in proliferating preadipocytes but disappear once they reach confluency (Gregoire et al., 1998; Rosen et al., 2002). *In vitro* and *in vivo* studies with double knock out for C/EBPδ and C/EBPβ provided varying results. The expression levels of both C/EBPα and PPARγ were found to be normal in double knock out mice, whereas a reduced expression of both C/EBPα and PPARγ was found in cells lacking both C/EBPδ and C/EBPβ. These findings suggest that, in addition to C/EBPδ and C/EBPβ, there may be other factors that allow PPARγ and C/EBPα expression *in vivo*. Other studies have shown that both C/EBPβ and C/EBPα can induce PPARγ expression in preadipocytes. C/EBPα transcription has been shown to be autoactivated. C/EBPα ectopic expression was able to induce adipogenesis without the need for an external adipogenic inducer (Rosen et al., 2002). C/EBPα knockout mice had lower adiposity. Even though C/EBPα is important for adipogenesis, it cannot function without PPARγ. Ectopic expression of C/EBPα in PPARγ -/- fibroblasts cannot induce adipogenesis, whereas ectopic expression of PPARγ in C/EBPα -/- cells can induce adipocyte differentiation but not insulin sensitivity. These findings indicate that mutual cooperation between C/EBPα and PPARγ is required for adipocyte differentiation and function (Gregoire et al., 1998; Rosen et al., 2002).

1.7.2 Other adipogenic transcription factors

SREBP-1c is another transcription factor that plays a role in PPARγ activation and adipocyte differentiation. It is a transcription factor in the basic helix loop helix leucine zipper family. SREBP-1c is abundant in the ATs and has been linked to adipogenesis (Gregoire et al., 1998). SREBP-1c overexpression in 3T3-L1 cells speeds up adipogenesis by activating PPARγ. However, SREBP-1c cannot induce adipogenesis by itself, and it has been demonstrated that

SREBP-1c facilitates adipogenesis by direct activation of PPARγ or by producing endogenous PPARγ ligands (Rosen et al., 2002).

Krüppel-like factors (KLFs) promote early adipogenesis by increasing the expression of C/EBPδ and C/EBPβ. Krüppel box 20 (Krox 20) has been shown to stimulate adipogenesis by upregulating C/EBPβ expression (Z. Wu & Wang, 2013). During adipogenesis, the early B-cell factor transcription factor family is expressed. Although liver X receptors are known to play a role in adipocyte differentiation, the precise mechanism has yet to be determined. Other transcription factors involved in adipogenesis include the signal transducer and activator of transcription-5a (STAT5a), the cyclic AMP response element-binding protein (CREB), the endothelial PAS domain-containing protein 1 (EPAS1), and the brain and muscle Aryl hydrocarbon receptor nuclear translocator (arnt) -like protein-1 (BMAL1) (Farmer, 2006; MacDougald & Lane, 1995).

1.8 Current strategies for prevention and treatment of obesity

The three main components of obesity prevention, management and/or treatment are non-pharmacological treatment (lifestyle modification), pharmacotherapy, and surgery (Figure 1.3) (Gadde et al., 2018). Behavioral interventions such as healthy diet and exercise will remain relevant to successful prevention of obesity. However, pharmacotherapy will continue to be crucial due to the growing prevalence in global obesity (Velazquez & Apovian, 2018).

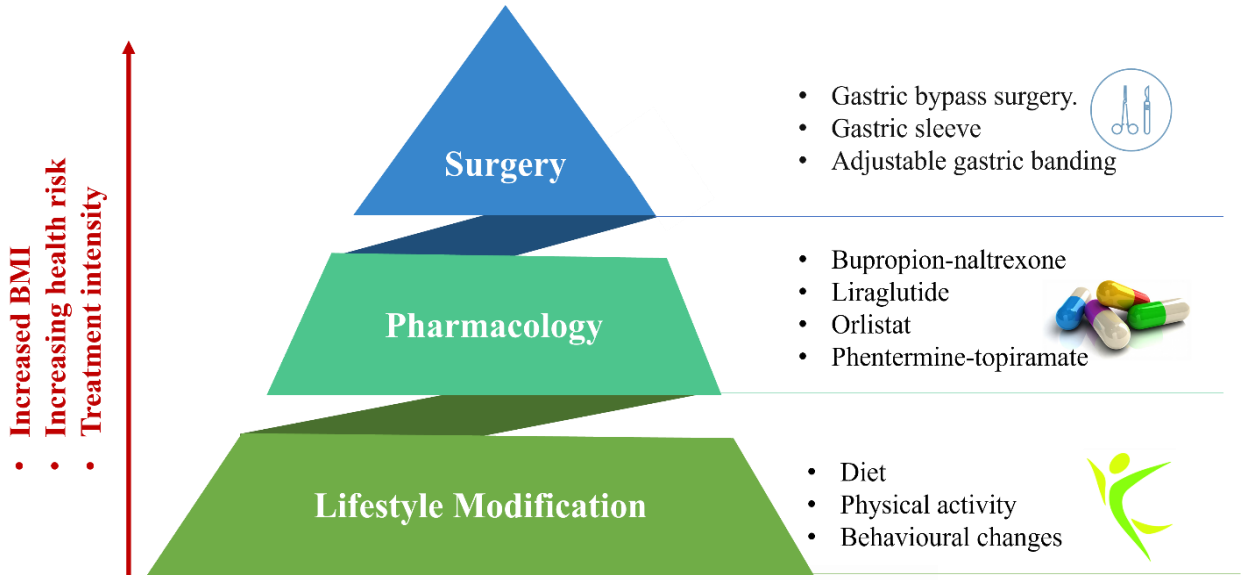

Figure 1.3: Examples of current strategies for prevention and treatment of obesity

There have been numerous attempts to treat the metabolic imbalance associated with obesity, leading to the development of a number of pharmacological drugs including, sibutramine, and orlistat. Pharmacological approaches to weight loss are divided into two categories: appetite suppressants and nutrient absorption inhibitors. Phentermine derivatives and sibutramine are two appetite suppressants (Bays et al., 2022). Orlistat is currently the only nutrient absorption inhibitor on the market. It can prevent up to 30% of fat absorption (Bansal & Khalili, 2022). The recommended drugs had an average weight loss ranging from 5 to 10% of the initial bodyweight. However, weight loss medications have not been particularly effective in the treatment of obesity to date, mainly due to their adverse effects (Bays et al., 2022).

Bariatric surgery, such as gastrointestinal Roux-en-Y bypass, has been shown to be the only clinically effective long-term weight loss strategy. Due to the complications that frequently necessitate additional follow-up surgery, this procedure is often reserved for morbidly obese patients with comorbidity as a last resort. Following surgery, the risk of obesity-related comorbidity and mortality is significantly reduced, particularly death from T2D, CVD, and

certain types of cancers (Crossan & Sheer, 2022). Given these encouraging results, alternative treatment strategies that can also promote effective and long-term weight loss, in a similar manner as surgical interventions are urgently needed for all patients.

1.9 AuNPs-based therapy as alternative treatment for obesity

Nanotechnology emerges as a useful technology to improve conventional therapeutic approaches and currently being explored in nanomedicine. Nanomedicine is defined as the use of nanomaterials at the nanoscale level in medical applications for disease prevention, diagnosis, monitoring, and treatment. Progress in the field of nanomedicine has had a significant impact on healthcare and has evolved alongside growing technological needs such as drug delivery (Sibuyi et al., 2018), *in vitro* diagnostics (Ou et al., 2019), *in vivo* imaging (Thovhogi et al., 2018a), therapy techniques (Phui & Ng, 2016; Yi et al., 2020), and tissue engineering (Zheng et al., 2021).

Richard P. Feynman gave a presentation titled "There's Plenty of Room at the Bottom" at the 1959 American Physical Society meeting in California, which sparked interest in nanotechnology (Feynman, 1960). The ability to manipulate matter at an incredibly small scale, often between 1 and 100 nm, provides many advantages that bulk counterparts do not have. At this size, physical laws can be applied differently for tangible benefits in various applications, such as the ability to deeply penetrate tumors, areas that are inaccessible to individual molecules or bulk solids, including conventional medicines (Hofmann-Amtenbrink et al., 2014). Particle size, shape, and surface properties have been linked to both drug pharmacokinetics and molecular pharmacodynamics. Molecules that were previously discarded due to biopharmaceutical constraints are now being used in the development of

effective nanoparticle-based therapeutics (Kim et al., 2010). Furthermore, the production of materials at this scale frequently yields unique and desirable chemical, physical, and biological properties (Khan et al., 2019).

Following the Food and Drug Administration's (FDA) clinical approval of Sandimmune®, a micellar drug for human administration in 1983, many drug nanoformulations have been systematically accepted for use in medicine (Ramanathan & Helderman, 2001). Table 1.2. presents a short summary of some of the approved nanomedicines. Currently, it is proposed that 100 nanotechnology-based bio-diagnostic or therapeutic systems, such as micelles, liposomes, dendrimers, inorganic NPs, and polymer-drug nanoconjugates, have been approved for clinical use to date, with over 563 in clinical trials and other developmental stages (Shan et al., 2022). However, the current study will focus on the use of AuNPs in the treatment of obesity.

Table 1.2: Summary of the approved nanomedicines in clinical use.

Nanoparticle	Indication	Product name	Company
		Organic NPs	
Micelles	Hormone replacement therapy	Estrasorb	Novavax; Bausch Health;
	Dry eye, Immunosuppression	Nanomicellar cyclosporine	Auven Therapeutics
	Ovarian Cancer	Apealea	Elevar Therapeutics
	Cancer	Doxophos	Oasmia Pharmaceutical
Liposomes	Fungal infections	Abelcet	Sigma-Tau
	Fungal/protozoal infections	AmBIsome	Gilead Sciences, Astellas Pharma
	Postoperative analgesia	DepoDur	Pacira Pharmaceuticals
	Atherosclerosis, Dyslipidemia	Inclisiran	Alnylam Pharmaceuticals
	Pancreatic cancer	Onivyde	Ipsen Biopharmaceuticals
Dendrimers	Bacterial vaginosis	Betadine BV	Starpharma
Polymers	Hyperkalemia	Veltassa	Amgen
	Dermatitis	Tropazone	Hi-Tech Pharmacal
	MRI contrast agent	Sirius	University of Texas System
	Crohn's disease, arthritis, ankylosing spondylitis	Cimzia	UCB
	Hepatitis B, hepatitis C	Pegasys	Genentech
	Osteoarthritis knee pain	Zilretta	Flexion Therapeutics
	Multiple sclerosis	Plegridy	Biogen
	Gout	Diafer	Duke University
		Inorganic NPs	
Iron oxide	Iron deficiency in CKD	Dexferrum	American Regent
	Iron deficiency in CKD	Infed	Actavis Pharma
Gold-coated silica	Acne vulgaris	Sebacia Microparticles	Sebacia
Superparamagnetic	Imaging, magnetic resonance	Feraheme	AMAG Pharmaceuticals

1.9.1 Biomedical applications of AuNPs

Michael Faraday published the first synthesis of colloidal gold, which is AuNPs in suspension, in 1857, long before peer-reviewed literature existed. He was the first to describe "ruby gold," a brilliant ruby suspension containing very fine AuNPs formed by the aqueous reduction of gold chloride by phosphorous and stabilized by the addition of carbon disulphide (Phui & Ng, 2016). Since then, advances in chemistry and physics have enabled the creation of AuNPs with precise control over particle size and shape distribution for a variety of applications (Khan et al., 2019). Although the Turkevich method is the extensively studied AuNPs synthesis method, its cytotoxic reducing agent and byproduct led to the innovative use of natural (plants and microorganisms) products as alternative reducing agents in green nanotechnology. All these methods are thoroughly reviewed elsewhere (Aboyewa et al., 2021; Sibuyi et al., 2021).

Among engineered inorganic nanomaterials, AuNPs have a high potential for biomedical applications as drug and gene delivery vehicles (Carvalho et al., 2019), photothermal (Lee et al., 2017), biosensors (Jafari & Hasanzadeh, 2020), diagnostic, and as contrast agents in various imaging techniques such as photoacoustic, computed tomography, Raman, differential interference contrast, and dark field microscopy (Ou et al., 2019). Their biomedical application is encouraged by the fact that bulk gold is a bioinert metal. Gold's nobility stems from its density, low toxicity in comparison to other metals, and extremely high thermal/electric conductivity. Unlike bulk gold or ionic gold, AuNPs has distinct electrical, chemical, mechanical, thermal, and optical properties (Alkilany et al., 2013; Sasidharan & Monteiro-Riviere, 2015). AuNPs have a high chemical stability compared to other metallic NPs, a narrow control of size or shape distribution during synthesis, easy surface functionalization, and high biocompatibility (Sharma et al., 2015; Yeh et al., 2012).

The medical properties of AuNPs are increasingly recognized, and explored as both therapeutic and viable drug delivery systems capable of addressing the non-selectivity and bystander toxic effects of conventional therapies (Shittu et al., 2017; Sibuyi et al., 2021). AuNPs-based formulations in pre-clinical and clinical trials include point-of-care diagnostics such as lateral flow assays; *in vivo* imaging and therapeutics (Figure 1.4). As an example, AuNPs in photothermal therapy, are able to absorb light in the near-infrared region for thermal ablation of solid tumors, the AuNPs will convert the energy of the photons into local heat that triggers apoptosis and/or necrosis of cancerous cells (Han & Choi, 2021). Furthermore, the ease of surface modification allows for the conjugation of therapeutic, targeting, and stabilizing agents on their surface; to prolong blood circulation and promote accumulation at pathological regions (Riley & Day, 2017). As a result, AuNPs have been used as drug carriers for chemotherapeutics (Riley & Day, 2017), immunomodulatory agents, and gene therapy (Wang et al., 2022), among others for treatment of various diseases including obesity (Sibuyi et al., 2018).

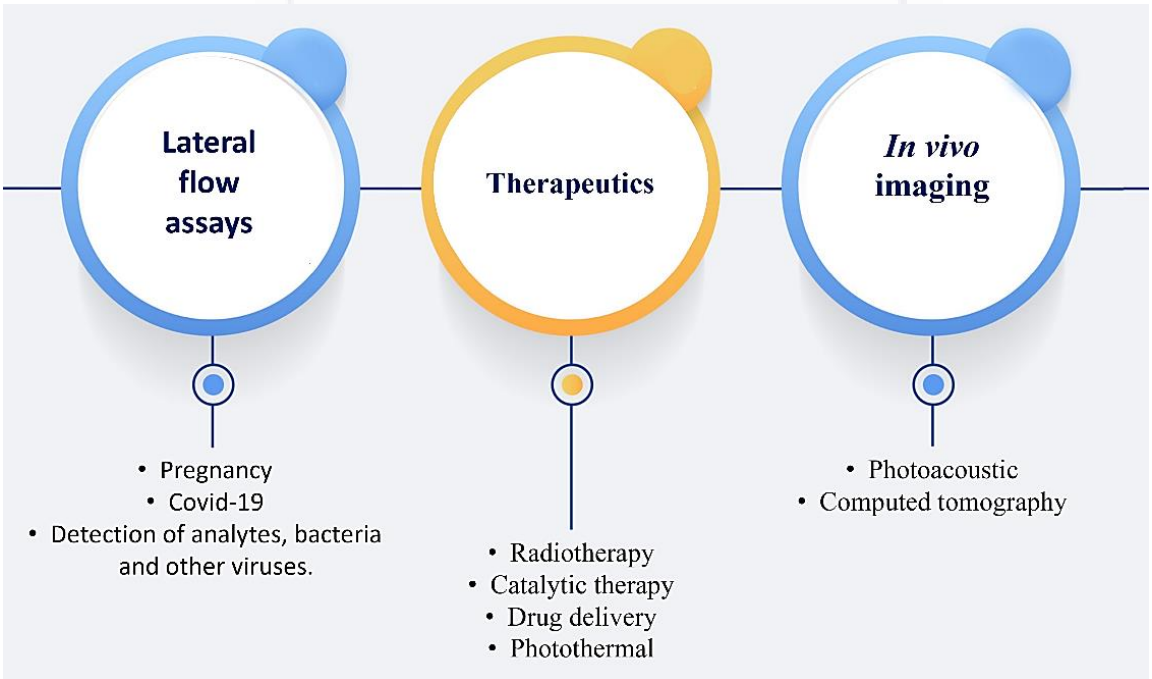

Figure 1.4: Examples of biomedical applications of AuNPs in pre-clinical and/or clinical setting.

1.9.2 AuNPs in obesity treatment

The role of AuNPs in obesity therapy has been reported. AuNPs were shown to be effective as potential drug delivery agents for anti-obesity drugs (Thovhogi et al., 2015), photosensitizers that can generate heat when irradiated by lasers in photothermal therapy (Ho Lee et al., 2017), and as therapeutic agents capable of reducing AT weight in treatment of obesity (Sibuyi et al., 2019). Table 1.3 presents several AuNPs-based nanotherapeutics that demonstrated anti-obesity properties. In a study by Chen et al., cAuNPs with a diameter of 21 nm were shown to significantly reduce abdominal fat accumulation and alleviate hyperlipidemia on high-fat diet (HFD) fed mice. Furthermore, poor glucose tolerance was reduced after intraperitoneal injection when compared to the untreated control group. The underlying mechanism was related to its ability to reduce macrophage recruitment and activity in AT and liver, as well as the secretion of pro-inflammatory cytokines and Tumour necrosis factor (TNF)-α, all of which are associated with obesity-related complications (Chen et al., 2018). Further research on mice with pre-existing obesity revealed that the cAuNPs treatment had a similar benefit, implying that cAuNPs have a promising future in the treatment of obesity and obesity-induced glucolipid metabolism disorders (Chen et al., 2018).

Table 1.3: Recent developments in AuNPs-based therapeutics and their therapeutic roles in the management of obesity and obesity-related metabolic complications

AuNPs	AuNPs size	Study model and experimental methods	Findings	Reference
Gynostemma pentaphyllum (GP)-AuNPs	20 - 200 nm	Differentiated 3T3-L1 and RAW 264.7 cells treated with GP-AuNP (3.125 µg/mL, 12.5 µg/mL and 50 µg/mL) for 8 days.	↓ intracellular lipid accumulation and TG content ↓ ROS production ↓ PPARγ and C/EBPα expression ↓ TNF-α expression	Akter et al. 2022
Smilax glabra (Sg)-AuNPs	50 - 90 nm	Diet induced obese and streptozotocin induced diabetic Wistar rats were orally dosed with Sg-AuNPs (50 mg/kg bwt) once a day for 15 days.	↓ BMI and body weight ↓ blood glucose ↓ liver marker enzymes and inflammatory markers	Ansari et al. 2019
cAuNPs	21 nm	Diet induced obese C57Bl/6 mice were injected with cAuNPs (0.785 µg Au/g (low dose) and 7.85 µg Au/g (high dose)) daily for 9 weeks.	↓ body weight and abdominal fat accumulation ↓ blood lipid levels ↓ hyperlipidemia ↑ glucose tolerance ↓ macrophage recruitment and activity in adipose tissue and liver ↓ secretion of pro-inflammatory cytokines and TNF-α	Chen et al. 2018
Salacia chinensis (Sc)-AuNPs	20 - 50 nm	Diet induced obese Wistar rats treated with ScAuNPs (10 mg/kg, 20 mg/kg and 30 mg/kg bwt) for 6 weeks.	↓ BMI and body weight, adipose index, leptin, and resistin ↑ adiponectin levels ↓ TC, FFA, LDL-C, TG, and VLDL-C levels ↑ HDL-C level ↓ CRI and AI levels ↓ liver marker enzymes and inflammatory markers ↓ AMPK1a levels ↑ pAMPK1a levels	Gao et al. 2020

Table 1.3: Recent developments in AuNPs-based therapeutics and their therapeutic roles in the management of obesity and obesity-related metabolic complications (continued)

AuNPs	AuNPs size	Study model and experimental methods	Findings	Reference
Poria cocos - AuNPs	20 nm	Wistar rats on HFD and streptozotocin induced diabetes were treated with Pc-AuNPs (25 mg/kg and 50 mg/kg bwt) once a day for 30 days.	↓ BMI and weight gain ↓ blood glucose, lipid metabolism, adipose tissue inflammation and oxidative stress ↑ satiety hormones ↓ cholesterol levels, atherogenic and coronary risk index, liver marker enzymes and inflammatory markers ↓ leptin and resistin ↑ adiponectin levels	Li et al. 2020
Panax ginseng - AuNPs	10 - 20 nm	3T3-L1 preadipocytes were differentiated to mature adipocyte in the presence of Pg-AuNP (10 µg/mL and 100 µg/mL) for 8 days. Matured 3T3-L1 adipocytes treated with Pg-AuNPs (100 µg/mL)	↓ intracellular lipid accumulation and TG content ↓ ak2, STAT3, PPARγ, CEBPα, CEBPβ, ap2, SREBP1c and FAS.	Simu et al. 2018
Dendropanax morbifera Léveille leaves -AuNPs	10 - 20 nm	Differentiated 3T3-L1 preadipocytes in the presence of D-AuNP (100 µg/mL) for 8 days. FFA-induced hepatic model HepG2 cells with D-AuNPs (100 µg/mL) treatment for 24and 48 hrs. FFA-induced hepatic model HepG2 cells with D-AuNPs (100 µg/mL) co-treatment for 24 hrs.	↓ intracellular lipid accumulation and TG content ↑ increased cholesterol inhibition ↓ adipogenic genes Jak2, STAT3, PPARγ, CEBPα in 3T3-L1 cells and ap2 expression levels in HepG2 cells ↓ fatty acid and acetyl coA expressed at HepG2 cells ↑ PPARα gene expression	Yi et al. 2020

Abbreviations: TG – triglycerides; HepG2 - human hepatoma; Jak2 - Janus kinase two; STAT3 - Signal transducer and activator of transcription three; PPAR - Peroxisome proliferator-activated receptor; CEBP - CCAAT enhancer-binding proteins, coA - Coenzyme A; FFA – Free fatty acids; ROS – Reactive oxygen species; TNF – Tumour necrosis factor; BMI – Body mass index; ak2 - adenylate kinase two, SREBP - Sterol regulatory element binding proteins, CRI – Coronary risk index; TC – Total cholesterol; LDL-C - low-density lipoprotein cholesterol; VLDL-C – very low-density lipoprotein cholesterol, levels, HDL-C – high density lipoprotein cholesterol; bwt – body weight

Green synthesized AuNPs using medicinal plants were also reported to have anti-obesity effects. *Smilax glabra* AuNPs (Sg-AuNPs) with various pharmacological properties such as anti-diabetic, anti-jaundice, and anti-cancer activities, also demonstrated anti-obesity effects in obese rats. The Sg-AuNPs significantly reduced weight of obese and streptozotocin-induced diabetic rats, aiding in the repair of hepatocytes and cardiac veins, and controlling weight gain at a dose of 50mg/kg body weight (Ansari et al., 2019).

AuNPs synthesized with *Poria cocos* (Pc-AuNPs), a saprophytic fungus used in Chinese and Japanese traditional medicine, reduced body weight and BMI on HFD-induced obese and streptozotocin diabetic rats after a 30 day treatment with 25 mg/kg and 50 mg/kg bwt of Pc-AuNPs (Li et al., 2020). Biochemical analysis confirmed that it may regulate glucose and lipid metabolism, as well as inhibit AT inflammation. Overall, the study demonstrated that Pc-AuNPs is a promising anti-obesity agent that not only prevents obesity but also obesity-related metabolic disorders (Li et al., 2020).

Another study examined anti-obesity effects in HFD-induced obese rats using *Salacia chinensis*-loaded AuNPs (Sc-AuNPs). Body weight, BMI, adipose index, leptin, resistin, atherogenic index, coronary risk index, liver marker enzymes, lipid profile, inflammatory markers, and adenosine monophosphate-activated protein kinase alpha 1 (AMPK1) were all reduced by Sc-AuNPs. Concurrently, Sc-AuNPs treatment increased adiponectin, high-density lipoprotein cholesterol, and phospho-AMPK 1 (pAMPK1). Histopathological test revealed improved anatomical features with reduced hepatocyte degradation after Sc-AuNPs treatment. The study showed that Sc-AuNPs act by regulating the serum lipid profile and the level of hormones related to lipid metabolism, as well as the transcriptional factors primarily responsible for the metabolism of lipid digestion and lipid accumulation, simultaneously improving metabolic markers related to coronary heart disease risk, among others. Thus, obesity-related metabolic improvements may contribute significantly to a lower risk of T2D,

obesity-related metabolic disorders, and an acute coronary event in high-risk patients (Gao et al., 2020).

The potential benefits of AuNPs synthesized from *Dendropanax morbifera Léveille* leaf extracts (D-AuNPs) on lipid accumulation was investigated on 3T3-L1 differentiated adipocytes and HepG2 Cells. The D-AuNPs demonstrated no cytotoxicity at concentrations up to 100 μg/mL. Furthermore, D-AuNPs treatment significantly downregulated expression of PPARγ, CEBPα, Jak2, STAT3, and ap2 adipogenesis-related genes in 3T3-L1 cells (Yi et al., 2020). Additionally, the D-AuNPs upregulated PPARα expression while also significantly downregulating the FAS and ACC levels in HepG2 cells. These findings suggested the anti-obesity effects of the D-AuNPS and potential of acting as cholesterol-lowering agents and improving other obesity related metabolic diseases including fatty liver disease (Yi et al., 2020).

Gynostemma pentaphyllum AuNPs (GP-AuNPs) was reported to reduce obesity and related inflammation. GP-AuNPs were not significantly toxic to RAW 264.7 cells and 3T3-L1 cells up to a concentration level of 100 μg/mL and 50 μg/mL, respectively. GP-AuNPs reduced lipid accumulation and suppressed TG content in 3T3-L1. The lipid-lowering effect was associated to downregulation of PPARγ and C/EBPα genes, which are important markers for cellular responses related to adipocyte differentiation and lipid accumulation. Reactive oxygen species (ROS), NO level, and TNF-expression which are major indicators of inflammation, were also significantly reduced. These findings demonstrated that GP-AuNPs have the potential to reduce obesity and obesity-related inflammation (Akter et al., 2022).

Panax ginseng (Pg-AuNPs) exerted significant anti-obesity properties in 3T3-L1 adipocytes and were not cytotoxic to the cells. Treatment with the Pg-AuNPs significantly inhibited intracellular TG and lipid accumulation in 3T3-L1 cells. Additionally, the expression of the

various adipogenic genes and signaling pathways including PPARγ, C/EBPα, SREBP1c, Jak-STAT3 and WNT were attenuated by Pg-AuNPs (Simu et al., 2018). Taken together, these findings suggest that Pg-AuNPs could be used as a novel therapeutic agent for the prevention and treatment of obesity.

Previous independent studies also showed that AuNPs can be functionalized with anti-obesity agents and used in targeted treatment of obesity. Targeted AuNPs-based strategies demonstrated enhanced selectivity and efficacy by targeting disease-specific biomarkers. Prohibitin (PHB) is one of the receptors that is overexpressed in the vasculature of WAT in obese humans, monkeys and rodents; and was investigated as a potential biomarker for obesity. Biomolecules functionalized with adipose homing peptide (AHP), a ligand that binds to PHB, were shown to target and kill PHB-expressing cells (Hossen et al., 2012; Kolonin et al., 2004). The adipocytes supported by these cells were starved and forced to metabolized the excess energy, leading to a reduction in fat mass. Further experiments demonstrated that the systemic administered PHB targeted-liposomes were selectively taken up by the AT vascular endothelial cells through PHB-mediated endocytosis leading to their death by apoptosis and significantly suppressed the progression of diet-induced obesity in mice (Hossen et al., 2012). The approach motivated the Biolabels Research Node (BRN) in using AuNPs as drug-delivery systems using the same targeting (AHP) and therapeutic (KLA) peptides for the treatment of diet-induced obesity in rats (Sibuyi et al., 2022).

The BRN have over the years explored AuNPs-based therapeutics for the reversal of obesity in *in vitro* (Sibuyi et al., 2017; Thovhogi et al., 2015), *in vivo* and *ex vivo* studies (Thovhogi et al., 2015), using the 14 nm cAuNPs as drug delivery vehicles. The cAuNPs were functionalized with AHP alone or in combination with $_{D}(KLAKLAK)_2$ as a therapeutic peptide (Sibuyi et al., 2017; Thovhogi et al., 2015). AHP-functionalized AuNPs were able to recognize and bind with

high specificity to PHB receptor in the WAT of obese subjects (Kolonin et al., 2004) and Caco-2 cells (Sibuyi et al., 2017; Thovhogi et al., 2015). The PHB-targeted AuNPs demonstrated specificity and $_{D}(KLAKLAK)_{2-}$ induced apoptotic cell death only on cells that express PHB receptor on the surface (Sibuyi et al., 2017; Thovhogi et al., 2015). *In vivo*, the AHP-AuNPs (Thovhogi et al., 2015) and AHP-functionalized quantum dots (Thovhogi et al., 2018a) were targeted at the AT vasculature of the obese rats. This suggested that the PHB-targeted nanotherapy can be used to reduce WAT mass, reverse obesity and restore the WAT physiological processes by inhibiting angiogenesis.

All these findings indicate that AuNPs-based obesity treatment options have potential, and more research is required before these materials can be used in clinical settings to prevent and treat obesity. The previous studies on AuNPs-based therapies were conducted on AuNPs with modified surfaces or cAuNPs with a 21nm diameter. The reluctance in using cAuNPs is based on hotly debated cytotoxicity or biological impact of these NPs. Numerous studies have found no adverse biological effects in either *in vitro* or *in vivo* experiments (Chithrani et al., 2006), and it has been suggested that some observed effects are due to substances conjugated to or adsorbed on their surface (Alkilany & Murphy, 2010), rather than the metal core of the AuNPs. Under certain conditions, cAuNPs have been shown to be cytotoxic, inhibit cell proliferation, anti-angiogenic, reduce the level of ROS, bind to or interact with biomolecules (proteins, amino acids, DNA), act as an effective adjuvant, or cause changes in cell morphology (Aillon et al., 2009; Alkilany & Murphy, 2010). Therefore, drawing conclusions from previous findings is difficult because each study used different-sized AuNPs with different surface coatings and shapes. In most cases the results are contradictory, some studies concluded that AuNPs were not toxic, while others concluded that their toxicity is attributed to their physicochemical properties. Although AuNPs have a promising future in mainstream clinical practice, the

biological environment is very complex, and NP interaction with biological components can result in NP transformation such as aggregation, resulting in the formation of large, irregularly shaped clusters (Moore et al., 2015). This phenomenon will significantly alter *in vitro* behavior as well as their fate *in vivo* which are mostly influenced by their physicochemical properties which will alter their reactivity, biodistribution, pharmacokinetics, cellular uptake, resulting in undesirable bystander effects (Augustine et al., 2020). As a result, there is an increasing need to effectively assess the nanomaterial-cell interactions in a cell/tissue and application-specific context, as well as to broaden knowledge on their toxicity and biocompatibility.

1.10 Cellular uptake and toxicity of AuNPs

AuNPs interaction with cellular components in the biological system such as membranes, mitochondria, nuclei, and proteins are critical in the execution of biomedical functions as well as toxicity. The discovery and/or design of new therapeutic agents require thorough knowledge of the processes involved between AuNPs and cells to help predict any possible NPs toxicological consequences *in vivo*. AuNPs' size, shape, and surface charge all play a role in their biological activities by facilitating their cellular uptake and internalization, which may result in cellular toxicity (Xia et al., 2019). Spherical AuNPs are said to be easier for cells to internalize and uptake than rod-shaped particles (Carnovale et al., 2019). NP size also has a significant impact on their intracellular uptake, with smaller NPs having higher uptake than larger ones. For example, 5 nm AuNPs have been shown to penetrate cells and bind to DNA irreversibly, whereas AuNPs with a diameter of 20 and 50 nm did not show cytotoxicity in both cancer cells and normal cells (Xia et al., 2019). AuNPs with either a positive or negative charged surface are highly reactive and cytotoxic to cells, causing mitochondrial oxidative stress (Alkilany & Murphy, 2010; Xie et al., 2017).

Cellular uptake of cAuNPs has been observed without significant cytotoxicity. AuNPs ranging from 4 to 18 nm and surface modified with various capping agents including citrate were found to be nontoxic in a human leukemia cell line (Connor et al., 2005). On RAW264.7 macrophage cells, 3.5 nm cAuNPs produced similar results. Here, the AuNPs were presumably taken up via endocytosis and were non-toxic to the cells with reduced ROS levels (Shukla et al., 2005). Villiers et al. investigated toxicity of 10 nm cAuNPs in dendritic cells and were also non-toxic. Moreover, the cAuNPs did not activate cells or alter the cell phenotype (Villiers et al., 2010). Cytotoxicity of the AuNPs, can also be cell specific depending on the receptors targeted by the NPs. For instance, 13 nm cAuNPs were toxic to a human carcinoma lung cells but not to a human liver carcinoma cells at the same concentrations (Patra et al., 2007). Furthermore, it is challenging to compare these studies because of the different dosing parameters and duration of AuNPs' exposure to cells.

Despite the extensive literature on *in vitro* cytotoxicity of AuNPs, cellular response to their exposure might vary significantly. While the cAuNPs might be considered as biocompatible following mitochondrial enzyme activity (tetrazolium tests) or phenotypic (microscopic) tests, genotoxicity might not be immediate and be reflected through altered gene expression. Therefore, it is critical to carefully examine the intracellular uptake pathways of NPs and cellular responses. This might be able to help unfold the potential signaling pathways activated by interactions of NPs with cells before detrimental effects manifests.

1.11 Rationale of study

In a previous study from our group, 14 nm spherical cAuNPs were investigated for their genotoxicity in the human colorectal adenocarcinoma (Caco-2) cells using analysis Mouse

Adipogenesis RT^2 Profiler PCR Array (Qiagen, Hilden, Germany). We found that the cAuNPs induced no notable changes in genes that are associated with genotoxicity in the Caco-2 cells, however, the expression levels of genes related to lipid metabolism were significantly altered. This suggested that the cAuNPs might have the potential to exert anti-obesity effects. Though there are several studies describing the anti-obesity effects of AuNPs, very little efforts have been made to understand the basic molecular mechanism of the process at the molecular level more so with unmodified AuNPs. Citrate has been shown to have a dual effect, acting as both a capping and a reducing agent; and the resulting cAuNPs have high affinity for thiolated biomolecules thereby improving the pharmacological efficacy and stability of unmodified AuNPs. Therefore, the current study investigated the effect of 14 nm cAuNPs and the molecular mechanism related to adipogenesis in mature 3T3-L1 adipocytes.

1.12 Study specific aim(s) and objectives

The aim of the study was to investigate the cytotoxic and anti-obesity effects of cAuNPs in 3T3-L1 cells at the molecular level.

The objectives were:

i) To synthesize and characterize 14nm cAuNPs

ii) To evaluate the cytotoxicity effects of the cAuNPs on differentiated and undifferentiated 3T3-L1 cells

iii) To evaluate the anti-obesity effects of the cAuNPs on the differentiated 3T3-L1 cells *in vitro*

iv) To examine effects of cAuNPs on mRNA expression levels of genes related to adipogenesis and lipid metabolism on differentiated, cAuNPs treated 3T3-L1 cells.

1.13 Hypothesis

Treatment of 3T3-L1 differentiated adipocytes with 14 nm cAuNPs will reduce lipid content on the cells by suppression of genes involved in adipogenesis.

CHAPTER 2: MATERIALS AND METHODS

2.1 Synthesis and characterization of cAuNPs

The synthesis of cAuNPs was carried out by citrate reduction of hydrogen tetrachloroarate ($HAuCl_4.3H_2O$) according to a previously described method (Sosibo et al., 2015). Briefly, 0.3 mM $HAuCl_4.3H_2O$ (Sigma, St Louis, USA) was added into hot distilled water (dH_2O) and vigorously stirred at 650 rpm for 2 min, followed by addition of 1% sodium citrate (Sigma). The heat was turned off after the solution changed colour, and continued to stir for another 60 min and allowed to cool at room temperature (RT). The cAuNPs were washed three times in dH_2O and characterized by the UV-visible (UV-vis) spectrophotometry (POLARstar Omega plate reader, BMG Labtech, Offenburg, Germany), High-Resolution Transmission Electron Microscope (HRTEM, FEI Tecnai G2, Oregon, USA), and Dynamic Light Scattering (DLS; Malvern Nano-ZS90 Zeta- sizer, Worcestershire, UK).

2.2 Determination of cAuNPs by UV-vis and ICP-EOS

The concentration of cAuNPs in solution was calculated according to the method described by Haiss et al. using Beer-Lambert's law (Haiss et al., 2007). The concentration of the cAuNPs, in a standard 1 cm path-length, was determined using the equation:

$$C = A450/\varepsilon 450$$

Where A is the absorption at 450 nm, and ε is the molar extinction coefficient at the wavelength of maximum extinction ($M^{-1}.cm^{-1}$).

The concentration of cAuNPs was further confirmed using inductively coupled plasma optical emission spectrometry (ICP-OES) on a Varian 710-ES ICP-OES (CA, USA) as previously described (Thovhogi et al., 2015). Briefly, 2mL cAuNPs were centrifuged at 14000 rpm for 5min at RT. The cAuNP pellets were then resuspended in 2mL Aqua regia solution (3:1 HCl: HNO3 (Kimix, Cape Town, South Africa) and digested by incubation at 90°C for 2 h. Thereafter the samples were diluted to 10ml with 2% HCl and analyzed using ICP-OES at the Chemistry Department (University of the Western Cape).

2.3 *In vitro* stability testing of cAuNPs

The *in vitro* stability of the cAuNPs was evaluated in different solutions as previously reported (Elbagory et al., 2019), with slight modifications. The cAuNPs were collected by centrifugation and re-suspended in 2 mL of five different solutions: 1 x Phosphate-buffered saline (PBS; Lonza, Verviers, Belgium), 10% Fetal bovine serum (FBS; Gibco, Mannheim, Germany), Dulbecco's modified eagle medium (DMEM/NC; Lonza), DMEM supplemented with 10% FBS and 1% penicillin-streptomycin (DMEM/C; Lonza); and dH_2O. After time intervals of 0 - 96 h incubation at 5% CO_2, 37 °C in a humified incubator (Thermo Electron Corporation, USA) and/or RT. The stability of the samples was evaluated by measuring the changes in UV-Vis spectra using the POLAR star Omega Microplate reader.

2.4 3T3-L1 cell culture

The 3T3-L1 mouse embryo fibroblasts were a kind gift from the Biomedical Research and Innovation Platform (South African Medical Research Council, Tygerberg, Cape Town), the cells were purchased from the American Type Culture Collection (Manassas, Virginia, USA).

The cells were cultured and maintained in DMEM/C in a 37°C humidified incubator with 5%CO_2 until >70% confluency.

2.4.1 Preadipocyte differentiation

The 3T3-L1 preadipocytes were seeded at a density of 3×10^4 cells/mL in 96 well culture plates. The differentiation process started after 48 h (day 0), the cells were stimulated to differentiate with DMEM/C containing a cocktail of hormones (MDI) that includes 0.5 mM IBMX (Sigma-Aldrich, Missouri, USA), 1 µM DEX (Sigma-Aldrich, Missouri, USA), and 1 µg/mL insulin (Roche, Germany) for two days following a previous protocol (Sung et al., 2011). Cells were then maintained in DMEM/C with 1 µg/mL insulin for another two days, followed by culturing with DMEM/C for an additional four days, at which time (day 10) cells were fully differentiated into mature adipocytes. To determine if there was auto differentiation of the pre-adipocytes without the presence of MDI induction media, the undifferentiated cells also followed the entire 10 day process maintaining the cells only in DMEM/C.

2.4.2 Cell viability analysis

The Water-soluble Tetrazolium, 2-(4-Iodophenyl)-3-(4-nitrophenyl)-5-(2,4disulfophenyl)-2H-tetrazolium (WST-1) assay (Roche, Germany) was used to assess the effects of cAuNPs on the viability of differentiated and undifferentiated 3T3-L1 cells. The test was carried out in accordance with the manufacturer's protocol, as described by Sibuyi et al (2017). In brief, the culture medium from the plates in 2.2.4.1 was replaced with 100 µl of cAuNPs prepared in DMEM at concentrations ranging from 0 - 400 nM and treated for 24 h, 48 h, and 72 h in three separate plates. The untreated cells served as the negative control. After respective incubation times, the treatment was removed and replaced with 100 µL of 1:10 WST-1 cell proliferation

reagent (5 mg/mL stock concentration) prepared in fresh media. Additional wells containing the same range of cAuNPs concentrations without the WST-1 were used to determine if there was interference of the cAuNPs with the assay. The plates were covered in foil and incubated at 37°C for 3 h. Absorbance was read at 440 nm using a PolarSTAR Omega plate reader with background subtraction at 630 nm. The cell viability was expressed as percentage cell viability of treated samples relative to the negative control cells, multiplied by 100.

2.4.3 Assessing intracellular lipid accumulation

Following treatment of 3T3-L1 cells with cAuNPs, intracellular lipid accumulation was assessed using Oil red O (ORO) and Crystal Violet (CV) staining on both differentiated and undifferentiated cells as previously described (Dludla et al., 2018). Following treatment, media was removed, and the cells were washed twice with PBS and then fixed with 10% (v/v) neutral buffered formalin for 15 min at RT. After the 10% formalin was removed, the cells were washed with PBS and incubated for 30 min with 50 µL 0.7% (v/v) ORO solution, including the background wells with no cells. The staining of lipid droplets in 3T3-L1 cells was removed and rinsed three times with dH_2O. Images of the cells were taken using an inverted microscope (EVOS XL Core imaging System microscope; Thermo Fisher Scientific, Germany). The ORO dye in the cells was extracted with 80 µL 100% isopropanol and the absorbance was measured at 490 nm using a POLARstar Omega plate reader.

CV stain was normalized to cell density as previously described (Dludla et al., 2018). Briefly, after reading absorbance of the ORO eluates, cells were washed with 70% ethanol (EtOH) once prior to incubation with 80 µL of CV 0.5% (v/v) for 5 min at RT. Cells were then washed 3 times with PBS. After that, to elute CV, 80 µL 70% EtOH was added to each well and gently swirled. Absorbance was then read at 570 nm.

The ORO stained images were analyzed by ImageJ software (Version 1.53, National Institute of Health, US). The region of interest was selected and measured by setting the colour threshold of the images based on hue, saturation, and brightness with the Colour Thresholding plugin. The results were expressed as a percentage of the ORO stained surface area. Each sample had three representative images analyzed, and means were used for comparison.

2.5 Real-time quantitative polymerase chain reaction (RT-qPCR)

2.5.1 RNA extraction

Cells were seeded at a cell density of 2 x 10^5 cells/mL in T25 cm^2 culture flasks and differentiated to mature adipocytes following the protocol described in 2.2.4**.** Thereafter, the medium was replaced with 5 mL DMEM/C containing 12.5 nM cAuNPs and the flasks were incubated for a further 24 h. The concentration (12.5 nM cAuNPs) used was adapted from our previous study which was shown to be not toxic to Caco-2 cells (Wusu et al., 2022). Untreated mature 3T3-L1 cells were used as reference or negative control.

At the end of the treatment, the media was removed, and the cells were rinsed with ice-cold PBS after which cells were lysed with RLT buffer and homogenized in the buffer containing a stainless steel bead for 2 min at 25 Hz using a Tissue lyser (Qiagen, Hilden, Germany) for RNA Extraction. Homogenization was repeated three times for 2 min in the Tissue Lyser with pre-cooled adapters and 1 min on ice. Homogenized cell lysates were centrifuged for 10 minutes at 15 000 × g at 4°C. The supernatant was transferred into a new 2 mL Eppendorf tube, 200 µL of chloroform was added, and the tube was centrifuged for 15 minutes at 15 000 × g and 4°C. The upper aqueous phase containing the RNA was transferred to a new 2 mL Eppendorf tube and 500 µL of isopropanol followed by incubation of the samples overnight at - 20°C to

precipitate the RNA. The samples were then centrifuged at 15 000 × g for 30 minutes at 4°C to pellet the RNA. The supernatant was discarded, and the RNA pellet was washed with 70% (v/v) EtOH and centrifuged at 15 000 × g for 15 minutes at 4°C. The wash step was repeated twice. After the final wash, EtOH was blotted from the Eppendorf tubes with a paper towel and the pellet was allowed to air dry. The RNA pellet was resuspended in 100 µL of RNase-free H_2O, pipetted up and down several times, and incubated at 55°C for 10 minutes to aid resuspension.

2.5.2 RNA quantification

RNA concentration and purity was determined using a NanoDrop One/Onec Microvolume UV-Vis Spectrophotometer (Thermo Scientific, Schwerte, Germany) and the concentration was further determined using Qubit™ RNA High Sensitivity (HS) and Broad Range (BR) Assay Kit (Life Technologies, Carlsbad, CA, USA) according to the manufacturer's protocol. Briefly, the Qubit™ working solution was prepared by diluting the Qubit® RNA HS Reagent in Qubit® RNA HS Buffer at 1:200. Then, 199 µL of the Qubit® working solution was added to 1 µL of RNA sample. RNA standards were prepared by adding 10 µL of the Qubit™ RNA Standard solutions to 190 µL Qubit® working solution. The assay tubes were briefly vortexed for about 5 s and then incubated at room temperature for 2 minutes. The Qubit® Fluorometer (Life Technologies) was fisrt calibrated with the RNA standards, followed by measuring the RNA concentrations in the RNA samples.

2.5.3 cDNA synthesis

The complementary DNA (cDNA) was synthesized using the RT^2 First Strand kit (Qiagen, Hilden, Germany) according to manufacturer's instructions. Briefly, 0.68 µg of total RNA was

combined with 2 µL gDNA elimination buffer (Buffer GE) and brought up to a final volume of 10 µL using RNAse-free H_2O. This mixture was incubated at 42 °C for 5 minutes and then chilled on ice. Thereafter, 10 µL of the Reverse-transcriptase mix containing recommended amounts of 5 x Buffer BC3, Control P2, RE3 Reverse Transcriptase Mix, and RNase-free H_2O were used was then added to this mixture and incubated at 42 °C for exactly 15 minutes followed by 5 minutes at 95 °C. Then, 91 µL RNase-free H_2O was added to each 20 µL cDNA synthesis reaction, and the diluted cDNA mixture was stored at −20 °C until used for gene expression profiling.

2.5.4 Adipogenesis RT^2 PCR array

RT-qPCR array analysis was performed in 96-well plates of a ready to use Mouse Adipogenesis RT^2 Profiler PCR Array (PAMM-049ZA; Qiagen) containing 84 genes related to the expression pattern of genes encoding pro/anti-adipogenic, pro/anti-WAT and pro/anti-BAT transduction pathways; 5 housekeeping genes and controls for RT and PCR reactions.

The cDNA samples from treated and untreated 3T3-L1 cells (2.2.5.3) were used as templates for the PCR array using RT^2 SYBR® Green qPCR Mastermix (Qiagen, Hilden, Germany). The PCR cocktail mixture was prepared on ice and contained 102 µL cDNA synthesis reaction, 1350 µL RT^2 SYBR® Green Mastermix, and 1284 µL RNase-free H_2O according to the manufacturer's instructions for a RT² Profiler PCR array 96-well format. Thereafter, a total volume of 25 µL of PCR master mixture - was pipetted into each well. The plates were pulse spun on a PlateFuge™ MicroPlate MicroCentrifuge (Benchmark Scientific) for 5 s.

RT-qPCR was conducted on the QuantStudio™ 3 Real-Time PCR System (Applied Biosystems, Foster City, CA, USA) at the Primate Unit and Delft Animal Centre (PUDAC, SAMRC, Delft, SA). The cycling conditions consisted of an initial 10 min step at 95°C,

followed by 40 cycles of 15 s at 95°C and 1 min at 60° C. PCR analysis data was conducted on the QuantStudio™ 3 Real-Time PCR System (Applied Biosystems, Foster City, CA, USA) at PUDAC and analyzed at GeneGlobe Data Analysis Center supplied by Qiagen.

2.5.5 Analysis of gene expression

Using the default baseline and cycle threshold (Ct) settings, the PCR array values were exported to an excel file, which was then uploaded to the manufacturer's web portal (http://www.qiagen.com/geneglobe). Target gene expression was normalized against the geometric mean based on manual selection of four housekeeping genes (beta-actin (ACTβ), Glyceraldehyde-3-Phosphate Dehydrogenase (GAPDH), beta-glucuronidase (GUSβ) and Heat Shock Protein 90 Alpha Family Class β Member 1 (HSP90AB1). The stability of the candidate reference genes was assessed by RefFinder algorithm based on four comprehensive methods including geNorm, Normfinder, BestKeeper, and comparative Delta-Ct, simultaneously. The normalized level of expression of the target gene in each sample was calculated using the ΔΔCT method. Ct values > 35 were excluded from the analysis and regarded as below the detection limit. Values were expressed as a fold of the control. Thus, genes were considered to be differentially expressed at a fold regulation threshold of 1.5 or greater, where significantly differentially expressed genes (DEGs) were defined to further have a p-value of ≤ 0.05.

2.5.6 Functional enrichment analysis of DEGs

To investigate the biological pathways and potential disease conditions among the DEGs, Kyoto Encyclopedia of Genes and Genomes (KEGG) pathway enrichment analysis was performed using the ShinyGo 0.77 web-based analysis application

(http://bioinformatics.sdstate.edu/go/). For the analysis, the significance of pathway enrichment was identified using a minimum false discovery rate (FDR) < 0.05.

2.5.7 Protein interaction network analysis of DEGs

The Search Tool for the Retrieval of Interaction Genes (STRING; https://string-db.org/) database was used to generate the protein-protein interaction after significantly DEGs were identified (PPI). A list of the DEGs that were significantly DEGs (n=6) was entered. The STRING database constructs a network of PPI from high-throughput experimental data, literature, and genomic context analysis predictions. STRING's interactions are derived from five major sources: genomic context predictions, high-throughput lab experiments, (conserved) co-expression, automated text mining, and previous knowledge in databases (Szklarczyk et al., 2023). The MCL clustering coefficient was set to 3 and the minimum required interactions score was set to high confidence (0.700).

2.6 Statistical analysis

The data are expressed as the mean ± standard error of mean (SEM) of three independent experiments. Statistical analysis was performed using GraphPad Prism v 6.1 software Comparisons between treatment groups were performed using one-way analysis of variance (ANOVA). The criterion was considered to be statistically significant when the p-value was < 0.05. The Bonferroni correction was used to compensate for multiple comparisons.

CHAPTER 3: RESULTS

3.1 Synthesis and characterization of cAuNPs

The cAuNPs with a diameter of 14 nm were reproduced using the citrate-reduction method previously described by Sosibo and colleagues (Sosibo et al., 2015), the cAuNPs properties were comparable to the cAuNPs in subsequent studies (Sibuyi et al., 2017; Sosibo et al., 2015; Thovhogi et al., 2015). The cAuNPs had a surface plasmon resonance peak of 521 nm (Figure 3.1(a)) determined from UV–VIS absorption spectrum and yielded an average hydrodynamic diameter size of 16.14 nm (Figure 3.1(b)), which could be attributed to the hydrodynamic capacity of citrate and H_2O surrounding the surface of the cAuNPs. The surface charge or the zeta potential (ζ-potential) of the cAuNPs was −28.7 mV (Figure 3.1(c)); the negative charge suggested that the cAuNPs were stable in solution (Nanocomposix, 2012). HR-TEM analysis revealed spherical cAuNPs (Figure 3.1(d)) with a core diameter of 14.20 nm (Figure 3.1(e)).

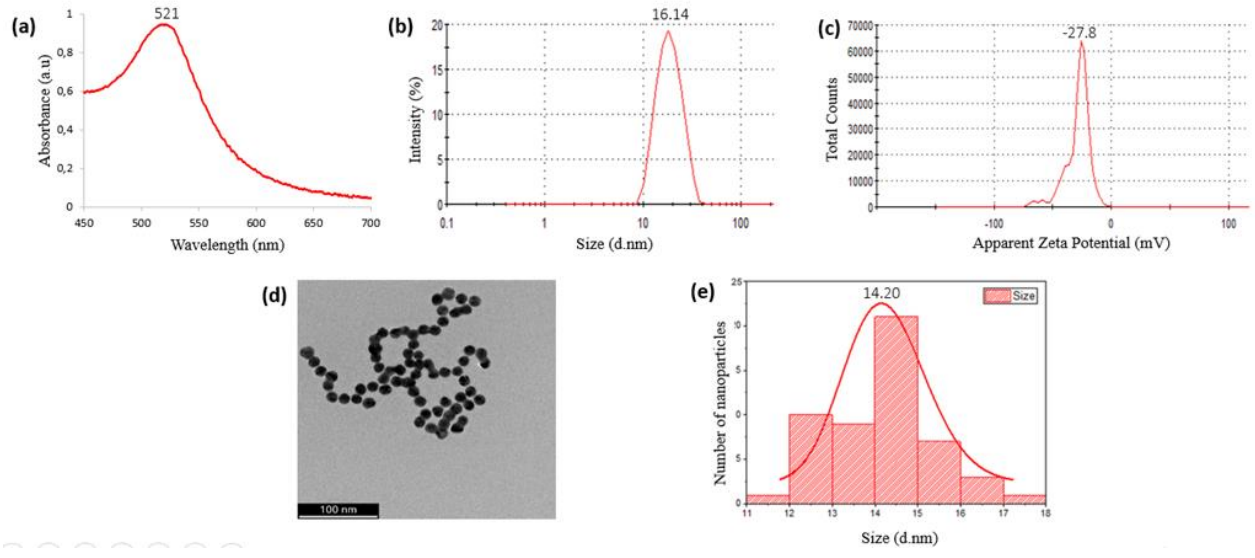

Figure 3.1: Physicochemical properties of the cAuNPs. (a) UV-vis spectrum, (b) hydrodynamic size from DLS, (c) Zeta potential, (d) HRTEM, and (e) core size distribution.

3.2 *In vitro* stability of cAuNPs

AuNPs must be stable in different biological media in order to be considered for biological applications. As a result, before proceeding with *in vitro* or *in vivo* studies, it is critical to investigate the stability of NPs in biological media and determine if NPs can retain their stability in biological environments (Phan & Haes, 2019). In this study, the stability of cAuNPs was assessed in dH_2O, DMEM/C, DMEM/NC, FBS, and PBS by investigating changes in the UV Vis spectra hourly for the first 6 h and at 6 h intervals thereafter for 96 h (Figure 3.2). The cAuNPs demonstrated that there were no significant changes in the independent stability in all solutions except for PBS. It is well known that cAuNPs colloids exhibit an abrupt change in colour from ruby red to purple upon dilution with PBS, and thus cannot be used in solutions with high salt content (e.g., PBS) or in the presence of high abundance proteins in biological milieu (e.g. albumin) (Phan & Haes, 2019). Thus, steric stabilization with molecules in such environments, such as peptides and polymers, is usually required to prevent ion binding and thus increase their bioavailability.

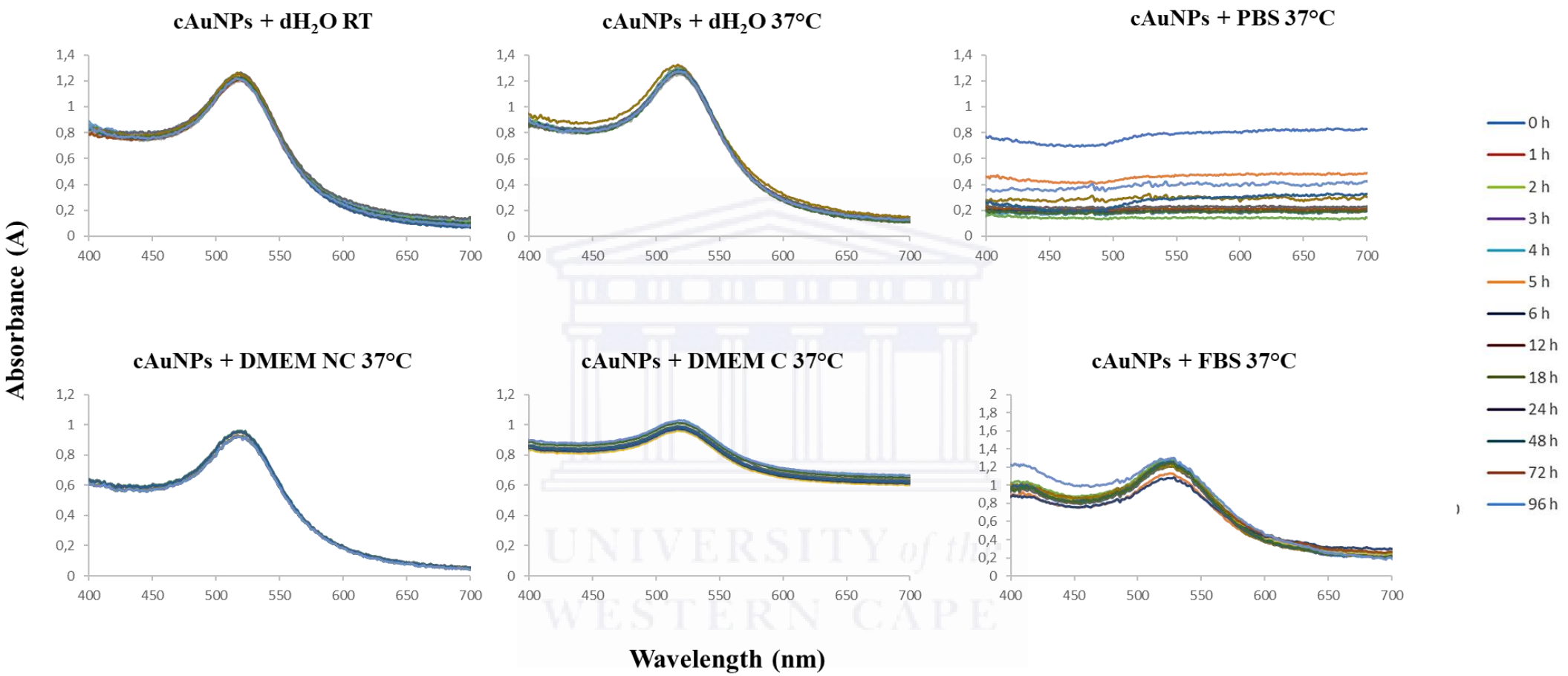

Figure 3.2*: In vitro* stability of cAuNPs in H2O, PBS, DMEM and FBS. UV-Vis spectra was monitored at 0 – 96 h after incubation in different solutions

3.3 Effects of cAuNPs on cell viability

Firstly, at day 10 post-MDI induction, the preadipocytes were fully differentiated to mature adipocytes. The results demonstrated that the obvious morphological phenotypes such as lipid droplets occurred during 3T3-L1 adipocyte differentiation, thus suggested that the cell model was achieved (Figure 3.3(a)). Undifferentiated 3T3-L1 cells that went through the 10 days in the absence of MDI remained without lipid droplets canceling out auto-differentiation and confirmed the model was successfully achieved (Figure 3.3(b)).

The effect of 14 nm cAuNPs on the viability of differentiated and undifferentiated mature 3T3-L1 cells was examined by WST assay, following incubation with increasing concentrations of the cAuNPs for 24 to 72 h. As shown in Figure 3.4, the cAuNPs showed no significant cytotoxicity or cell death at all the time points. The cell proliferation rates at 48 h (Figure 3.4(b)) and 72 h (Figure 3.4(c)) showed a negligible increase in the percentage of cell viability, especially for the undifferentiated cells. Thus, the cAuNPs up to 400 nM were not cytotoxic to both differentiated and undifferentiated 3T3-L1 cells (mature adipocytes).

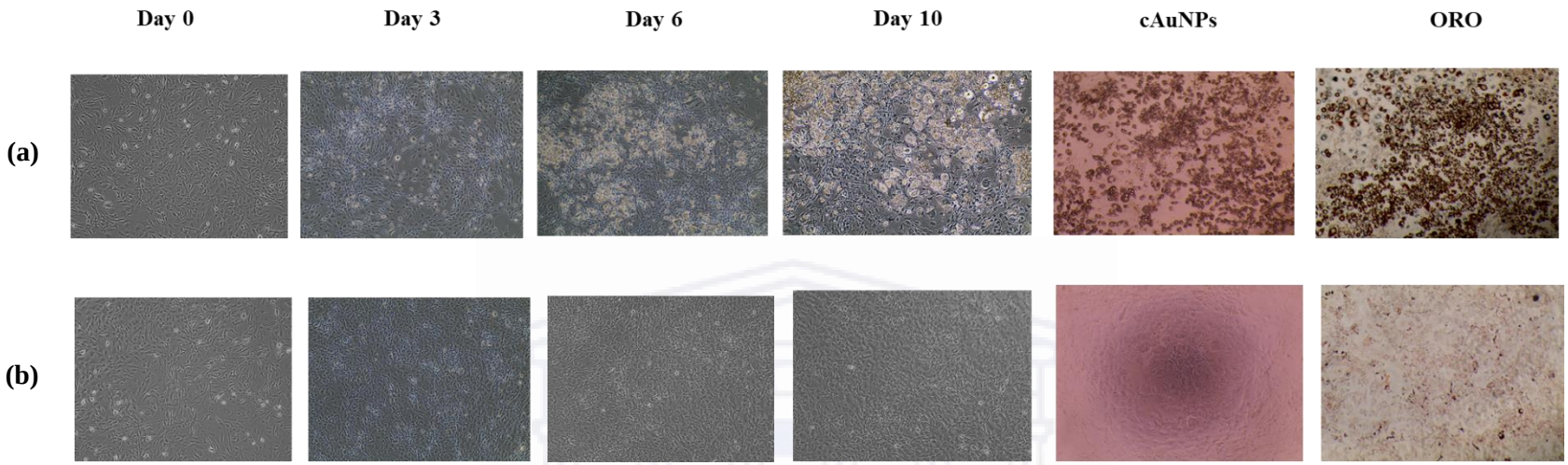

Figure 3.3: 3T3-L1 cell differentiation using MDI at 10X magnification. (a) Differentiated cells maintained in MDI differentiation cocktail consisting of 0.5 mM IBMX, 1 µM DEX, 1 µg/mL insulin; (b) Undifferentiated cells maintained in DMEM/C.

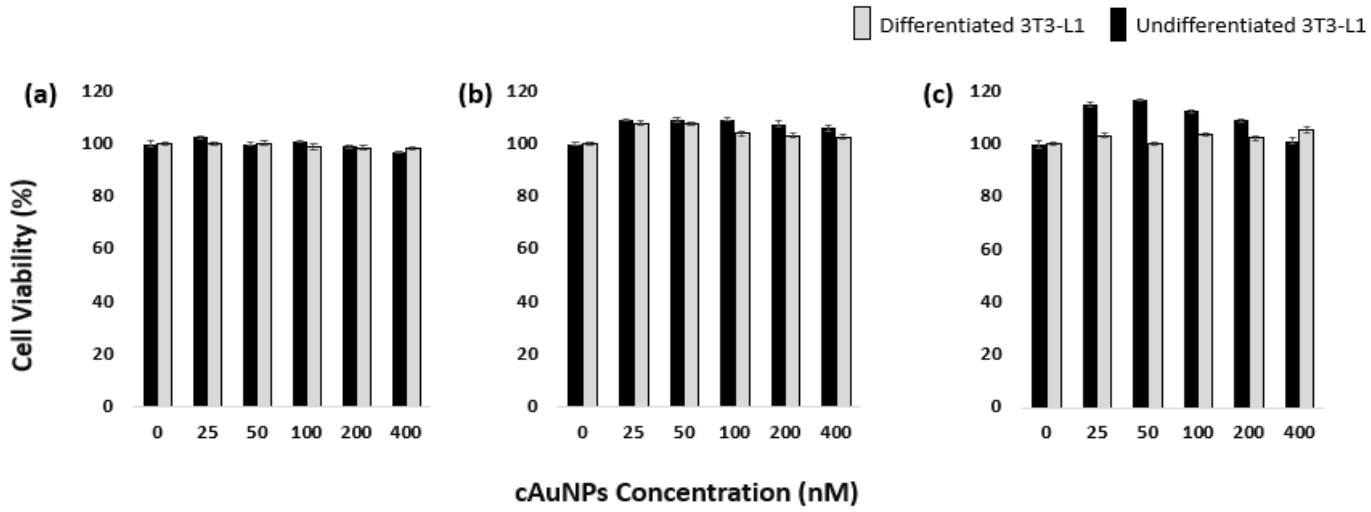

Figure 3.4: Effects of cAuNPs on differentiated and undifferentiated 3T3-L1 cell viability. 3T3-L1 cells, cultured in 96-well plates, were treated with a cAuNPs concentration between 0 and 400 nM for (a) 24 h; (b) 48 h; (c) 72 h; Cell viability was assessed using WST-1 assay. Data are presented as the mean ± SD of three independent experiments.

3.4 Effect of cAuNPs on intracellular lipid accumulation

To assess the effect of cAuNPs on the intracellular lipid accumulation, fully differentiated adipocytes and undifferentiated 3T3-L1 cells were treated with 0 - 400 nM of cAuNPs for 24, 48 and 72 h. Microscopic examination of cells stained with ORO revealed no visible differences in the lipid content of the cAuNPs-treated cells, as there were no clear differences on the ORO-stained lipid droplets (Figure 3.5). The results were quantified by measuring the absorbance of the solubilized stained lipid droplets at 490 nm. Figure 3.6 showed that the treatment with the cAuNPs resulted in a concentration-dependent reduction of lipid accumulation in the cells. Thus, amongst other factors like size, shape, surface charge, surface composition, and synthesis method, concentrations of the cAuNPs clearly depicted a dose-dependent effect on the cells (Aillon et al., 2009; Alkilany & Murphy, 2010).

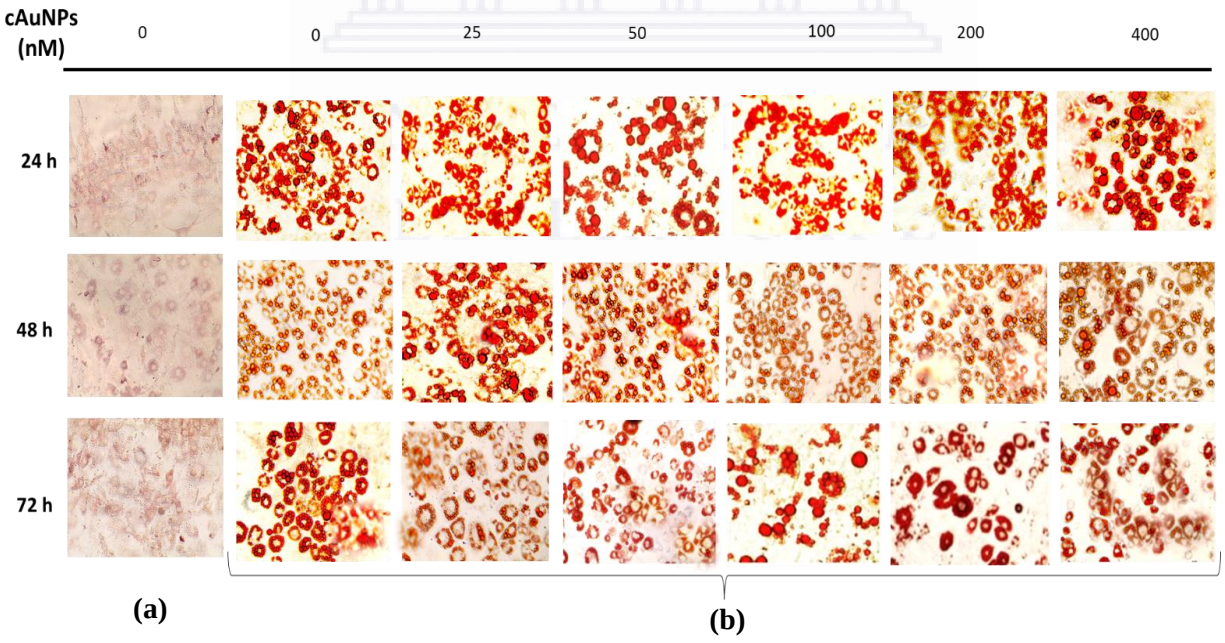

Figure 3.5: Effect of cAuNPs on 3T3-L1 cells lipid content stained by ORO dye at 40X magnification. (a) Undifferentiated 3T3-L1 adipocytes. (b) Differentiated 3T3-L1 adipocytes. Red colour represents lipid droplets quantifying intracellular lipid content. ORO: Oil Red O.

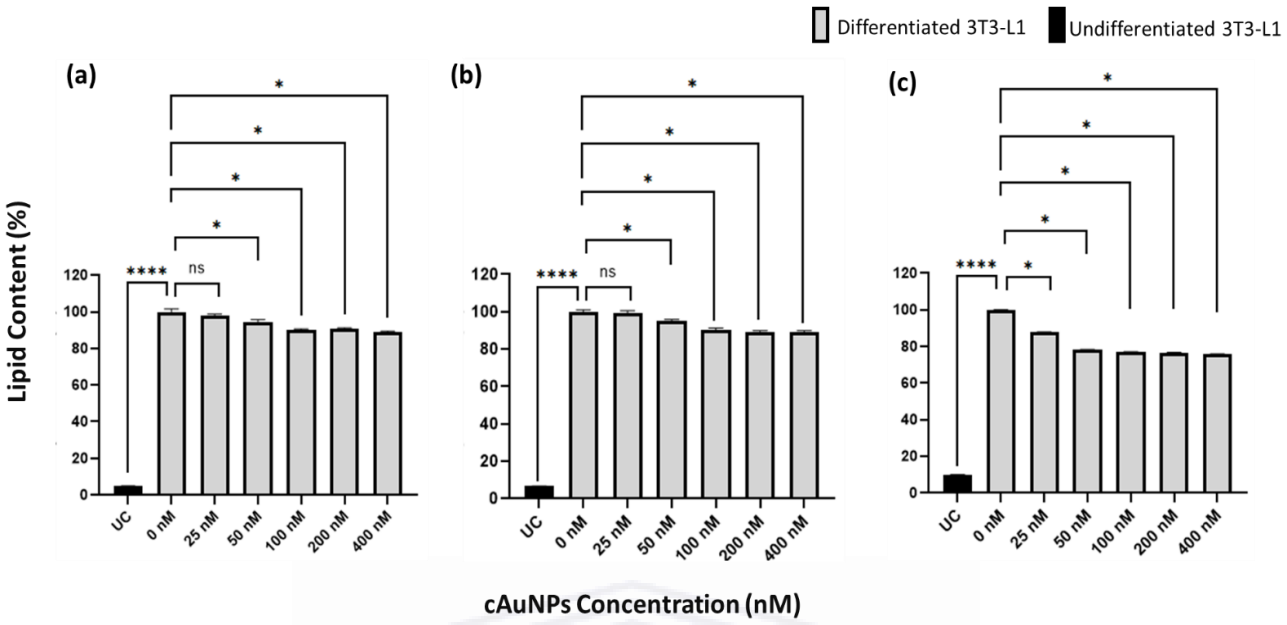

Figure 3.6: Effect of cAuNPs on 3T3-L1 cells lipid content stained by ORO dye quantitative representation. (a) 24 h. (b) 48 h. (c) 72 h. Data are expressed as mean ± S.E.M., (n=3). ****P < 0.0001, *P < 0.05 compared to untreated (UC). UC = Undifferentiated control

3.5 Effects of cAuNPs on Gene Expression Levels of adipogenic genes

The Mouse Adipogenesis RT^2 Profiler™ PCR Array was utilized to evaluate changes in gene expression, as a response to treatment of 3T3-L1 adipocytes with cAuNPs, compared to the untreated cells. The results were represented in a heatmap along with a gene clustering dendrogram, indicating linkage in the alteration profile (Figure 3.7).

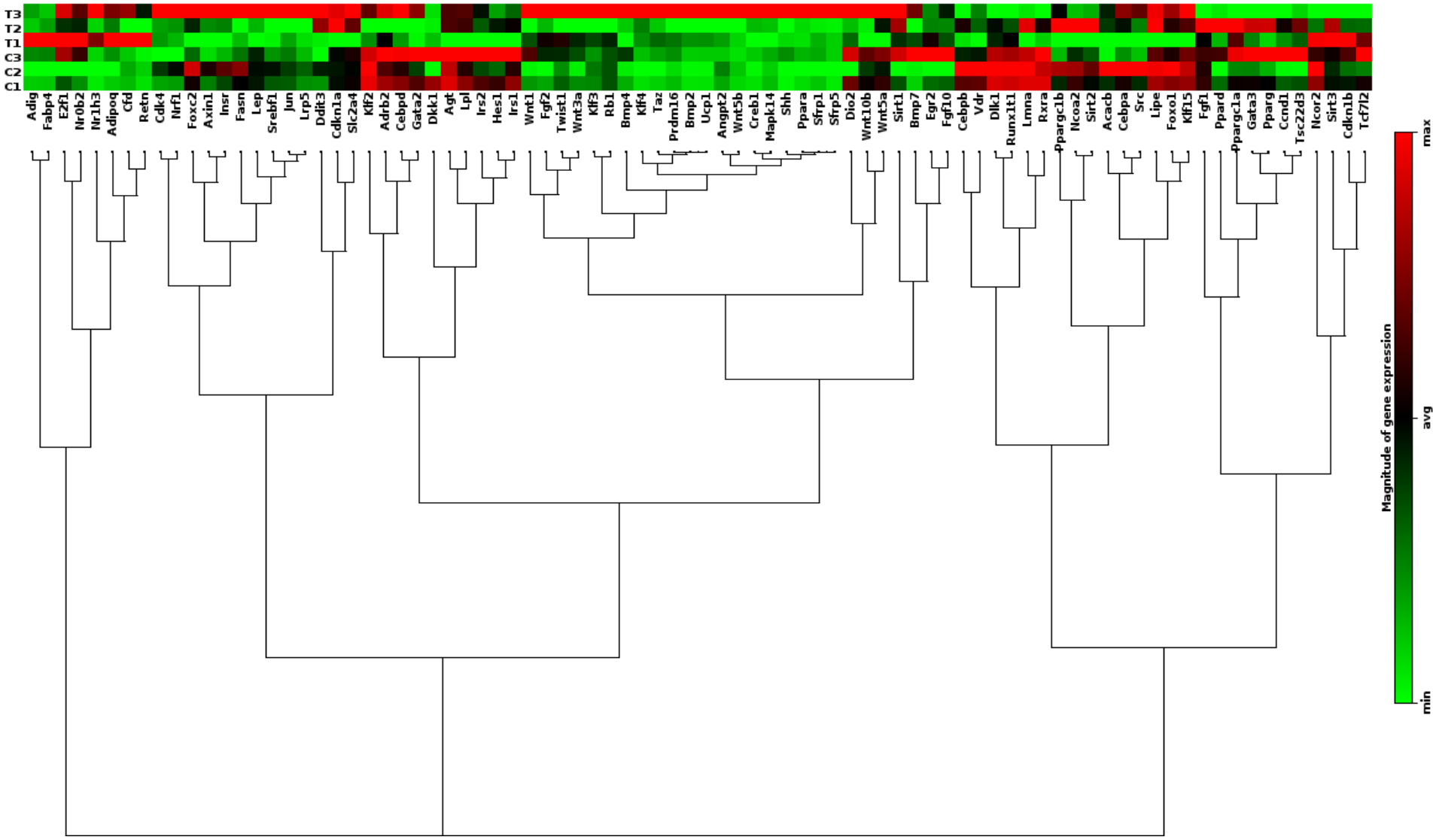

Figure 3.7: Heatmap of gene expressions and unsupervised hierarchical cluster analysis for genes involved in adipogenesis pathway comparing cAuNPs treated and untreated 3T3-L1 differentiated adipocytes. All data were normalized to the housekeeping genes; green = downregulated; red = upregulated; C = Control; T = Treatment.

The PCR array revealed that out of the 84 genes, the cAuNPs altered the expression of 35 genes (Figure 3.8, Table 3.1), where 18 of these genes were upregulated and 17 downregulated at a fold change greater than 1.5. The yellow and blue dots in Figure 3.8 represent the genes that were upregulated and downregulated, respectively.

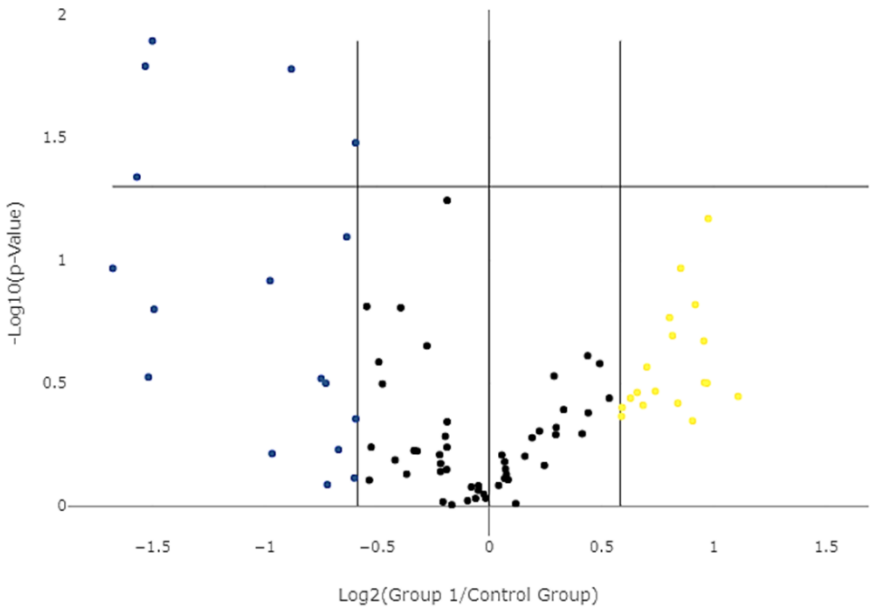

Figure 3.8: Volcano plot representing DEGs in 3T3-L1 differentiated adipocyte treated with 12.5 nM cAuNPs compared to the untreated cells. Yellow = up-regulated genes, blue = down-regulated genes and black = genes that did not change in expression levels.

Table 3.1: Upregulated and downregulated DEGs in 3T3-L1 differentiated cells treated with cAuNPs

Gene Description	Gene Symbol	p-value	Fold Regulation	Gene Function
	Upregulated			
Adipogenin	*Adig*	0.340652	1,67	Adipokines
Adiponectin, C1Q and collagen domain containing	*Adipoq*	0.067545	1,97	Adipokines; PPARγ Targets
Bone morphogenetic protein 2	*Bmp2*	0.315726	1,96	Pro-WAT
cAMP responsive element binding protein 1	*Crebp1*	0.363437	1,55	Pro-Brown Adipose Tissue
Complement factor D (adipsin)	*Cfd*	0.202290	1,76	Adipokines; PPARγ Targets
Fatty acid binding protein 4, adipocyte	*Fabp4*	0.344552	1,58	PPARγ Targets; Pro-Adipogenesis
Fibroblast growth factor 2	*Fgf2*	0.271385	1,63	Pro-Adipogenesis
Kruppel-like factor 4 (gut)	*Klf4*	0.170849	1,75	Pro-WAT
Nuclear receptor subfamily 0, group B, member 2	*Nr0b2*	0.151324	1,89	Anti-Brown Adipose Tissue
Nuclear receptor subfamily 1, group H, member 3	*Nr1h3*	0.107527	1,81	Anti-Brown Adipose Tissue
Peroxisome proliferator activated receptor alpha	*Pparα*	0.388582	1,61	Pro-Brown Adipose Tissue
PR domain containing 16	*Prdm16*	0.396812	1,51	Pro-Brown Adipose Tissue
Resistin	*Retn*	0.212713	1,94	Adipokines; PPARγ Targets
Secreted frizzled-related protein 1	*Sfrp1*	0.380933	1,79	Pro-Adipogenesis
Secreted frizzled-related protein 5	*Sfrp5*	0.357688	2,16	Pro-Adipogenesis
Sonic hedgehog	*Shh*	0.449580	1,87	Anti-Adipogenesis
Uncoupling protein 1 (mitochondrial, proton carrier)	*Ucp1*	0.314366	1,94	Pro-Brown Adipose Tissue
Wingless-related MMTV integration site 5B	*Wnt5b*	0.431093	1,5	Pro-Adipogenesis

Table 3.1: Upregulated and downregulated DEGs in 3T3-L1 differentiated cells treated with cAuNP (continued).

Gene Description	Gene Symbol	p-value	Fold Regulation	Gene Function
	Downregulated			
Adrenergic receptor, beta 2	*Adrb2*	0.302541	-1,68	Anti-Adipogenesis
Angiotensinogen (serpin peptidase inhibitor, clade A, member 8)	*Agt*	0.080173	-1,55	Hormones; PPARγ Targets
CCAAT/enhancer binding protein (C/EBP), beta	*Cebpb*	0.107633	-3,2	Pro-Adipogenesis
CCAAT/enhancer binding protein (C/EBP), delta	*Cebpd*	0.316031	-1,66	Pro-Adipogenesis
Delta-like 1 homolog (Drosophila)	*Dlk1**	0.016618*	-1,84	Anti-Adipogenesis
Dickkopf homolog 1 (Xenopus laevis)	*Dkk1*	0.157985	-2,81	Pro-Adipogenesis
Fibroblast growth factor 1	*Fgf1*	0.768058	-1,52	Pro-Adipogenesis
GATA binding protein 3	*Gata3*	0.588959	-1,59	Anti-WAT
Kruppel-like factor 2 (lung)	*Klf2**	0.033174*	-1,51	Anti-WAT
Lamin A	*Lmna*	0.120902	-1,97	Pro-Adipogenesis
Leptin	*Lep*	0.817793	-1,65	Adipokines
Nuclear receptor co-repressor 2	*Ncor2*	0.298549	-2,86	Anti-Adipogenesis
Retinoid X receptor alpha	*Rxra**	0.012760*	-2,83	Pro-Adipogenesis
Runt-related transcription factor 1; translocated to, 1 (cyclin D-related)	*Runx1t1**	0.016184*	-2,89	Anti-Adipogenesis
Transcription factor 7-like 2, T-cell specific, HMG-box	*Tcf7l2*	0.441263	-1,51	Anti-Adipogenesis
Vitamin D receptor	*VDR**	0.045728*	-2,97	Anti-Adipogenesis
Wingless related MMTV integration site 10b	*Wnt10b*	0.611492	-1,95	Anti-Brown Adipose Tissue

***Statistically significant at p<0.5**

Among which expression of 5 DEGs (*Dlk1, Klf2, Runx1t1, Rxra, VDR*) was significantly altered (Figure 3.9). The expression of these DEGs was downregulated Compared to the untreated cells. The functions of the altered genes (*Dlk1, Runx1t1, VDR*) as summarized in Table 3.1, were associated with anti-adipogenesis, while the other 2 genes (*Rxra* and *Klf2*) were involved in pro-adipogenesis and anti-WAT.

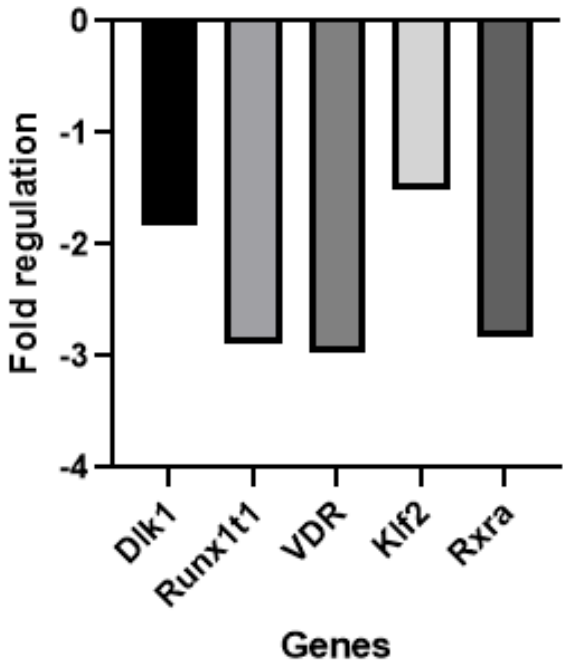

Figure 3.9: DEGs with statistically significant changes in gene expression, where $p < 0.05$ and fold change is 1.5 or greater

3.6 KEGG pathway analysis of the DEGs

To better understand the associated functions of the 5 downregulated DEGs in 3T3-L1 adipocytes (Figure 3.9), KEGG signaling pathway analysis of the DEGs was performed using ShinyGO tool. Function annotation showed that the DEGs were significantly enriched in 21 KEGG pathways involved in endocrine, cancer, excretory, digestive, immune, signal transduction, metabolic, cardiovascular and infectious disease system pathways (Figure 3.10).

Interestingly, numerous KEGG pathways indicated that diverse metabolic changes were occurring in the cancer-associated pathways. It was also revealed that 'Parathyroid hormone synthesis, secretion and action' was the most significantly enriched KEGG pathway.

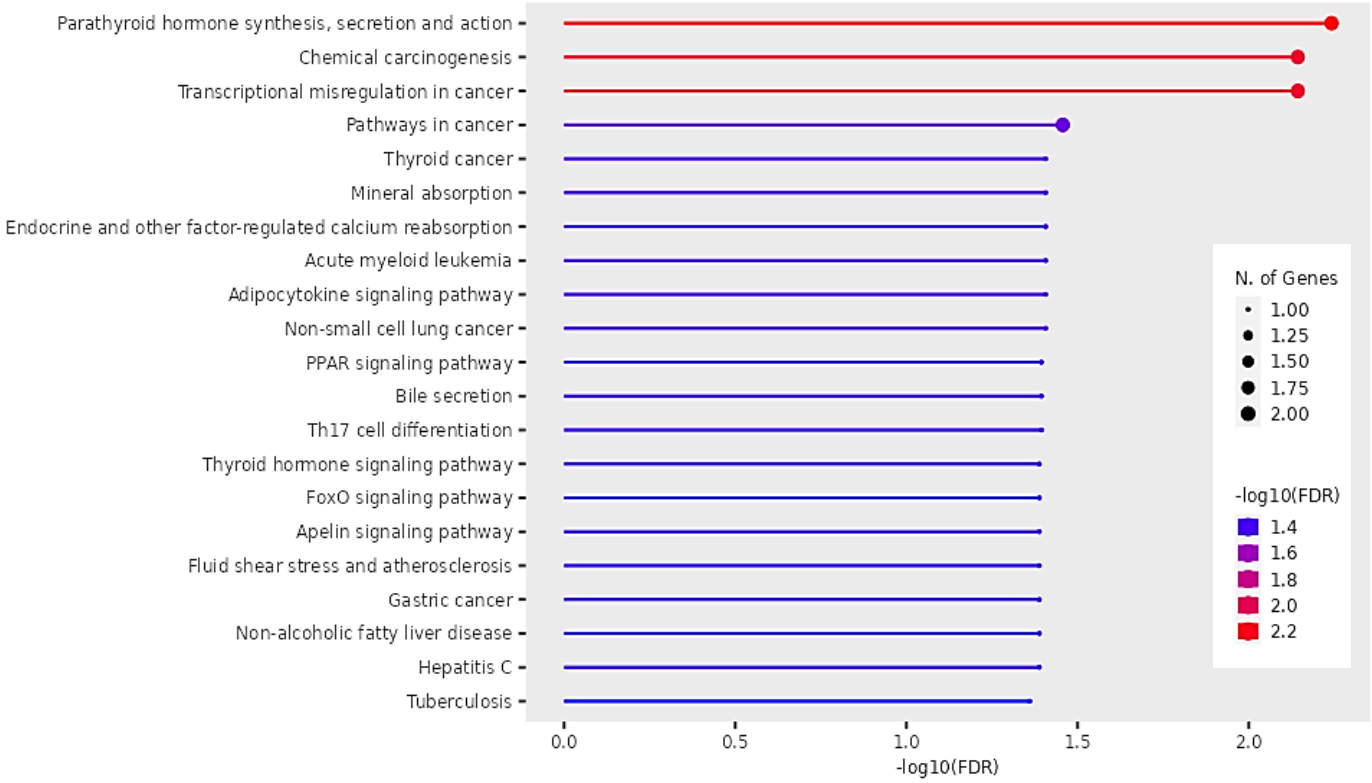

Figure 3.10: KEGG Classification of DEGs in cAuNPs-treated 3T3-L1 adipocytes.

3.7 Functional interactions of proteins encoded by DEGs

STRING, as previously reported, was used to investigate the interactions of proteins encoded by DEGs. The PPI network showed one protein-DEG interaction module (*Rxra* and *VDR*), while three DEGs (*Runx1t1*, *Dlk1* and *Klf2*) were unrelated to this protein interaction (Figure 3.11). The PPI enrichment p-value was 0.0188, indicating that no significant enrichment was discovered.

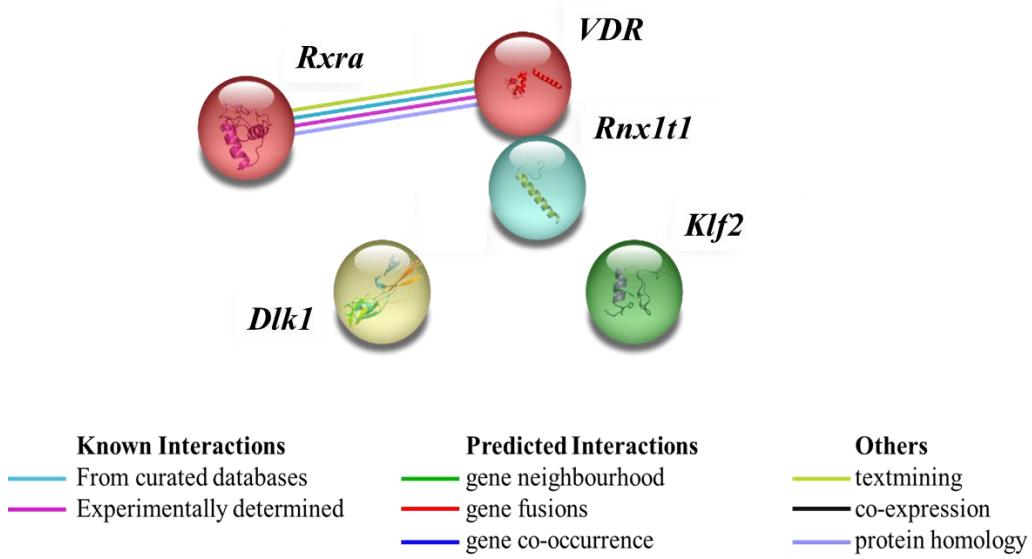

Figure 3.11: String representation of PPI network of the genes that were significantly differentially expressed in cAuNPs-treated 3T3-L1 adipocytes.

CHAPTER 4: DISCUSSION AND CONCLUSION

4.1 Discussion

The Biolabels Research Node have over the years explored AuNPs-based therapeutics for the reversal of obesity in *in vitro* (Sibuyi et al., 2017; Thovhogi et al., 2015), *in vivo* and *ex vivo* studies (Thovhogi et al., 2015), where 14 nm cAuNPs were used as drug delivery vehicles. In these studies, the cAuNPs were functionalized with AHP alone or in combination with a therapeutic or $_D(KLAKLAK)_2$ peptide (Sibuyi et al., 2017; Thovhogi et al., 2015). AHP-functionalized AuNPs bound with high specificity to PHB receptors on the cell surface of WAT vasculature of obese rats (Thovhogi et al., 2015) and Caco-2 cells (Sibuyi et al., 2017). The PHB-targeted AuNPs demonstrated high specificity by inducing $_D(KLAKLAK)_2$-apoptotic cell death only on Caco-2 cells (Sibuyi et al., 2017; Thovhogi et al., 2015). *In vivo*, the AHP-functionalized AuNPs (Thovhogi et al., 2015) and quantum dots (Thovhogi et al., 2018b) were targeted at the WAT vasculature of obese rats. This suggested that the PHB-targeted nanotherapy can be used to inhibit angiogenesis which will in turn reduce WAT mass, reverse obesity and restore the WAT physiological processes.

Interestingly, in another study the untargeted cAuNPs were reported to downregulate expression of genes involved in lipid metabolism (Table 4.1), in particular, 4 genes involved in steatosis (*SREBF1*, *SCD*, *PPARA*, *FASN*), 3 in phospholipidosis (*TAGLN*, *INHBE*, *HPN*), 2 in cholestasis (SLC51A, RDX), and 1 involved in fatty acid metabolism (CPT1B) (Wusu et al 2021). These findings, therefore suggested that the cAuNPs might have anti-lipogenic effect and possibly anti-obesity effects. Hence, the current study was purposed to study the effects of cAuNPs in an *in vitro* model of 3T3-L1 differentiated adipocytes to confirm their possible anti-obesity effects.

Table 4.1: Differentially expressed lipid metabolism genes in cAuNP treated Caco-2 cells adapted from Wusu et al (2021)

Gene symbol	Gene name	Function	Gene Pathway
SREBF1	Sterol regulatory element binding transcription factor 1	Controls the expression of genes involved in fatty acid and triglyceride synthesis (Sun et al., 2021).	Steatosis
SCD	Stearoyl-CoA Desaturase	Encodes an enzyme that participates in monounsaturated fatty acid biosynthesis, specifically oleic acid synthesis.	Steatosis
FASN	Fatty acid synthase	Catalyses the synthesis of long-chain saturated fatty acids (Jensen-Urstad & Semenkovich, 2012).	Steatosis
PPARA	Peroxisome Proliferator Activated Receptor Alpha	Key regulator of lipid metabolism (Stienstra et al., 2007)	Steatosis
TAGLN	Transgelin	Encodes a shape change and transformation sensitive actin-binding protein (Ritter et al., 2022)	Phospholipidosis
INHBE	Inhibin Subunit Beta E	Encodes a member of the transforming growth factor-beta (TGF-β) superfamily of proteins involved in the regulation of liver cell growth and differentiation (Sugiyama et al., 2018).	Phospholipidosis
HPN	Hepsin	Promotes liver metabolism while inhibiting adipocyte browning (S. Li et al., 2020).	Phospholipidosis
CPT1B	Carnitine Palmitoyltransferase 1B	Rate-limiting step of the long-chain fatty acid beta-oxidation pathway in muscle mitochondria (Maples et al., 2015)	Fatty acid metabolism
SLC51A	Solute Carrier Family 51 Subunit Alpha	Transporter responsible for bile acid export said to potentially affect multiple metabolic pathways in the pathophysiology of obesity (Haeusler et al., 2016).	Cholestasis
HPX	Hemopexin	Encodes a plasma glycoprotein with a high affinity for heme and transports it to the liver for breakdown and iron recovery. HPX expressed in adipose tissue participates in lipogenesis and adipogenesis and influences adiponectin expression.	Immunotoxicity

AuNPs possess a variety of biological activities that are attributed to their unique properties. AuNPs are the most extensively studied metal-based NPs with applications in a wide range of health conditions including cancer (Gavas et al., 2021), cardiovascular disease, diabetes (Phui & Ng, 2016), and obesity (Sibuyi et al., 2019). AuNPs have been shown to lower blood glucose, cholesterol, and weight gain in mice fed a high-fat diet (Ansari et al., 2019; Chen et al., 2018; Gao et al., 2020).

The present study gives an insight into the potential lipid lowering effects of cAuNPs on 3T3-L1 adipocytes and identity of some genes involved in this role. The study provide evidence that cAuNPs can inhibit lipid accumulation at lower dose (≤400 nM) compared to the reported doses used by similar studies (Akter et al., 2022; Chen, et al., 2018).

To elucidate the anti-obesity effect of cAuNPs, the accumulation of triglyceride (intracellular lipid content) was investigated on 3T3-L1 adipocytes. Triglyceride was inhibited in a dose-dependent matter of concentrations that was nontoxic to the cells (Figures 3.4 and 3.6). These results were consistent with those of previous (Akter et al., 2022; Simu et al., 2018; Yi et al., 2020). Additionally, the effects of cAuNPs were also consistent on the Caco-2 cells exposed to various concentrations of either cAuNPs (Thovhogi et al., 2015; Wusu et al., 2022) or peptide-functionalized cAuNPs (Sibuyi et al., 2018; Thovhogi et al., 2015). The cAuNPs were nontoxic to Caco-2 cells at lower concentrations (≤ 12.5 nM) (Sibuyi et al., 2017; Wusu et al., 2022). However, it has been observed that at higher concentrations, the Caco-2 cell viability might be impacted (Wusu et al., 2022).

The potential antiobesity effect of the cAuNPs was further confirmed by investigating expression profiles of genes involved in adipogenesis on 3T3-L1 differentiated cells. Genes that were found to be significantly downregulated (Figure 3.7 and Table 3.1) were involved in

anti-adipogenesis (*VDR*, *Dlk1*, and *Runx1t1*), anti-WAT (*Klf2*), and pro-adipogenesis (*Rxra*) molecular pathways.

VDR, a nuclear receptor for calcitriol, the active form of vitamin D3 that mediates its action on cells, is essential for calcium homeostasis. Furthermore, *VDR* modifies certain biological effects such as glucose and lipid metabolism, cell proliferation and differentiation, and immune cell activation. It has been demonstrated that diet-induced obese mice with increased *VDR* mRNA expression have higher levels of serum triglyceride and cholesterol than normal mice, implying a link between *VDR* gene expression levels and the development of obesity (Sirajudeen et al., 2019). Moreover, increased *VDR* expression suppresses the expression of UCP1, a protein that influences BAT thermogenic capacity (Calcium et al., 2011).

Dlk1 is one of four proteins that encode genes in the Dlk1-Dio3 domain that have been linked to important roles in adipogenesis and fat accumulation. The role of *D1k1* in obesity is complex, however, recent studies have suggested that *Dlk1* should be considered a factor causally linked to obesity and insulin resistance, and that it could be used as a therapeutic target or early biomarker for patients with T2D and cancer (Jensen et al., 2019).

Runx1t1 is an adipogenic gene that is thought to promote adipogenic differentiation by increasing D-type Cyclin genes (Cyclin D1 & D3) during mitotic clonal expansion in adipogenesis. Studies on Runx1t1 in obesity is limited, but has been extensively studied for its sophisticated functions since its discovery. It is as an important angiogenic driver for vasculogenesis in the formation of blood vessels. Previous research has shown that Runx1t1 has pleiotropic effects on fat development, such as inhibiting C/EBP activity during adipogenesis and significantly increasing the number of adipocytes (hyperplasia) in 3T3-L1 adipocytes via Runx1t1 alternative splicing (Deng et al., 2018). Studies have also suggested

that *Runx1t1* may be involved in the regulation of thermogenesis and energy expenditure, which could contribute to reduced lipid accumulation (Huang et al., 2011).

Anti-WAT gene, *Klf2,* a major regulator of adipogenesis, impose its functions by targeting PPARγ. Members of the Kruppel-like factor (KLF) family of zinc-finger transcription factors have recently been identified as key regulators of cell activity and have received intensive investigations in human health and disease. *Klf2* is mainly expressed in preadipocytes of WAT with the expression levels diminishing in mature adipocytes. Our study showed that *Klf2* was significantly downregulated in mature adipocytes. Similar to our findings, the expression of *Klf2* was significantly lowered in the mature adipocytes in response to the antiadipogenic effect of capsaicin (Baboota et al., 2014).

Rxra, a receptor for retinoic acid, is also known to have a role in insulin sensitivity, adipogenesis, and fat metabolism (Wu & Yin, 2022). However, *Rxra* studies were more focused on DNA methylation status in mother and child (Pant et al., 2020). In addition, *Rxra* serves as a common heterodimeric partner for a number of nuclear receptors including those that regulate gene expression in various biological processes (Wu & Yin, 2022).

Thus, the downregulated genes (*VDR*, *Dlk1*, *Runx1t1*, *Klf2*, and *Rxra*) in this study have all been implicated in the regulation of lipid metabolism, suggesting that reduced expression or activity of these genes may contribute to the reversal of obesity and obesity-relatated metabolic disorders.

Moreover, it should be noted that these genes' involvement in multiple physiological functions, as well as their reliance on various endogenous and exogenous factors, may contribute to the observed lack of correlation in STRING (Figure 3.11). For example, the significantly enriched top 3 KEGG pathways, namely: “parathyroid hormone synthesis, secretion and action”,

"transcriptional misregulation in cancer" and "chemical carcinogens" are notably all related to cancer. Interestingly, it has been reported that parathyroid hormone synthesis, secretion and action is also correlated with obesity. Parathyroid hormone (PTH) is a key regulator of calcium and phosphorus homeostasis, and it works by binding to the PTH/PTH-related peptide receptor (PTH1R). PTH1R primarily activates two heterotrimeric Gprotein subtypes, which regulate the activity of adenylyl cyclases and phospholipase C (PLC), which control the flow of cAMP/PKA and IP/PKC signaling cascades (Kulebyakin et al., 2022). Mesenchymal stem cells (MSCs) give rise to both adipocytes and osteoblasts. Increased adipocytes in the bone marrow have an inverse relationship with bone formation. Adipocytes in the bone marrow can influence osteoblastic activity and function, increase osteoclast activity, and impede bone mineralization (Adam et al., 2010). Romagnoli et al. demonstrated that abdominal fat accumulation has a negative impact on the microstructure of bone trabeculae (Romagnoli et al., 2016).

Subsequently, other studies have since shown that obesity may contribute to the development of Primary hyperparathyroidism (PHPT) via vitamin D deficiency and the resulting autonomous stimulation and growth of the parathyroid glands (Adam et al., 2010). This clearly shows that *VDR* expression may play a role in obesity promotion; however, acting as an independent gene, its downregulated expression may influence WAT browning and other antiadipogenic factors, including weight loss. PHPT, on the other hand, has been linked to the development of obesity. Indeed, some authors consider obesity to be a feature of PHPT due to the high prevalence of obesity observed in PHPT patients (Feng et al., 2022; Romagnoli et al., 2016).

4.2 Conclusion

The objectives of this study were to synthesize 14 nm cAuNPs, evaluate their potential antiadipogenic effects and related gene expression in 3T3-L1 adipocytes. The cAuNPs were synthesized by the citrate reduction method, with citrate acting as both the reducing and stabilizing agent. The 14 nm cAuNPs demonstrated low to no cytotoxic effects on both differentiated and undifferentiated 3T3-L1 cells, suggesting that the cAuNPs are biocompatible. Furthermore, the anti-obesity effects of 14 nm cAuNPs was investigated on 3T3-L1 differentiated adipocytes as an *in vitro* model of obesity. Although no significant changes were observed based on the ORO assay, the cAuNPs quantitively reduced the lipid content in a concentration-dependent manner. The PCR array results provide a foundation to further explore the molecular mechanisms and strong evidence that the cAuNPs had antiadipogenic effects through regulation of the genes mostly related in obesity development and progression. The results proved that the 14 nm cAuNPs have a potential application in the development of anti-obesity therapy and may provide hope in the management and treatment of obesity.

4.3 Study Limitations and Recommendations

Despite the study's significant findings, there were some limitations to be considered when using an *in vitro* model. *In vitro* studies may not accurately reflect the complexities of *in vivo* systems, which often produce contradictory results. Although the DEGs were previously implicated in obesity, further validation by qPCR, protein expression and post-transcriptional regulation following exposure to cAuNPs are recommended. Future studies should incorporate *in vivo* models to further validate the association of DEGs with the molecular mechanisms underlying the effects of cAuNPs. Furthermore, there is a need for a more targeted approach to

improve the specificity of cAuNPs in order to maximize their potential use in anti-obesity therapy. Nonetheless, this study provided a foundation for future research on the use of AuNPs-based therapeutic strategies as an option for management and treatment of obesity and obesity-related diseases.

REFERENCES

Aboyewa, J. A., Sibuyi, N. R. S., Meyer, M., & Oguntibeju, O. O. (2021). Green Synthesis of Metallic Nanoparticles Using Some Selected Medicinal Plants from Southern Africa and Their Biological Applications. *Plants*, *10*(9), 1929. https://doi.org/10.3390/PLANTS10091929

Adam, M. A., Untch, B. R., Danko, M. E., Stinnett, S., Dixit, D., Koh, J., Marks, J. R., & Olson, J. A. (2010). Severe Obesity Is Associated with Symptomatic Presentation, Higher Parathyroid Hormone Levels, and Increased Gland Weight in Primary Hyperparathyroidism. *The Journal of Clinical Endocrinology and Metabolism*, *95*(11), 4917. https://doi.org/10.1210/JC.2010-0666

Ahmad, B., Serpell, C. J., Fong, I. L., & Wong, E. H. (2020). Molecular Mechanisms of Adipogenesis: The Anti-adipogenic Role of AMP-Activated Protein Kinase. *Frontiers in Molecular Biosciences*, *7*, 76. https://doi.org/10.3389/FMOLB.2020.00076/XML/NLM

Aillon, K. L., Xie, Y., El-Gendy, N., Berkland, C. J., & Forrest, M. L. (2009). Effects of nanomaterial physicochemical properties on in vivo toxicity. *Advanced Drug Delivery Reviews*, *61*(6), 457–466. https://doi.org/10.1016/J.ADDR.2009.03.010

Akter, R., Ling, L., Rupa, E. J., Kyupark, J., Mathiyalagan, R., Nahar, J., Won, L. J., Hyun, K. Do, Murugesan, M., Yang, D. C., Kang, S. C., & Kwak, G. Y. (2022). Binary Effects of Gynostemma Gold Nanoparticles on Obesity and Inflammation via Downregulation of PPARγ/CEPBα and TNF-α Gene Expression. *Molecules*, *27*(9). https://doi.org/10.3390/MOLECULES27092795

Alkilany, A. M., Lohse, S. E., & Murphy, C. J. (2013). The gold standard: gold nanoparticle libraries to understand the nano-bio interface. *Accounts of Chemical Research*, *46*(3), 650–661. https://doi.org/10.1021/AR300015B

Alkilany, A. M., & Murphy, C. J. (2010). Toxicity and cellular uptake of gold nanoparticles: what we have learned so far? *Journal of Nanoparticle Research : An Interdisciplinary Forum for Nanoscale Science and Technology*, *12*(7), 2313–2333. https://doi.org/10.1007/S11051-010-9911-8

Ansari, S. A., Bari, A., Ullah, R., Mathanmohun, M., Veeraraghavan, V. P., & Sun, Z. (2019). Gold nanoparticles synthesized with Smilax glabra rhizome modulates the anti-obesity parameters in high-fat diet and streptozotocin induced obese diabetes rat model. *Journal of Photochemistry and Photobiology B: Biology*, *201*. https://doi.org/10.1016/J.JPHOTOBIOL.2019.111643

Audano, M., Pedretti, S., Caruso, D., Crestani, M., De Fabiani, E., & Mitro, N. (2022). Regulatory mechanisms of the early phase of white adipocyte differentiation: an overview. *Cellular and Molecular Life Sciences 2022 79:3*, *79*(3), 1–14. https://doi.org/10.1007/S00018-022-04169-6

Augustine, R., Hasan, A., Primavera, R., Wilson, R. J., Thakor, A. S., & Kevadiya, B. D. (2020). Cellular uptake and retention of nanoparticles: Insights on particle properties and interaction with cellular components. *Materials Today Communications*, *25*. https://doi.org/10.1016/J.MTCOMM.2020.101692

Baboota, R. K., Singh, D. P., Sarma, S. M., Kaur, J., Sandhir, R., Boparai, R. K., Kondepudi, K. K., & Bishnoi, M. (2014). Capsaicin Induces "Brite" Phenotype in Differentiating 3T3-L1 Preadipocytes. *PLoS ONE*, *9*(7), 103093. https://doi.org/10.1371/JOURNAL.PONE.0103093

Bansal, A. B., & Khalili, Y. Al. (2022). Orlistat. *XPharm: The Comprehensive Pharmacology Reference*, 1–3. https://doi.org/10.1016/B978-008055232-3.62333-5

Bays, H. E., Fitch, A., Christensen, S., Burridge, K., & Tondt, J. (2022). Anti-Obesity Medications and Investigational Agents: An Obesity Medicine Association (OMA) Clinical Practice Statement (CPS) 2022. *Obesity Pillars*, *2*, 100018. https://doi.org/10.1016/J.OBPILL.2022.100018

Calcium, I. of M. (US) C. to R. D. R. I. for V. D. and, Ross, A. C., Taylor, C. L., Yaktine, A. L., & Valle, H. B. Del. (2011). *Overview of Vitamin D*. https://www.ncbi.nlm.nih.gov/books/NBK56061/

Capelli, D., Cerchia, C., Montanari, R., Loiodice, F., Tortorella, P., Laghezza, A., Cervoni, L., Pochetti, G., & Lavecchia, A. (2016). Structural basis for PPAR partial or full activation revealed by a novel ligand binding mode. *Scientific Reports*, *6*. https://doi.org/10.1038/SREP34792

Carnovale, C., Bryant, G., Shukla, R., & Bansal, V. (2019). Identifying Trends in Gold Nanoparticle Toxicity and Uptake: Size, Shape, Capping Ligand, and Biological Corona. *ACS Omega*, *4*(1), 242–256. https://doi.org/10.1021/ACSOMEGA.8B03227/ASSET/IMAGES/MEDIUM/AO-2018-03227J_M004.GIF

Carvalho, A., Fernandes, A. R., & Baptista, P. V. (2019). Nanoparticles as Delivery Systems in Cancer Therapy: Focus on Gold Nanoparticles and Drugs. *Applications of Targeted Nano Drugs and Delivery Systems: Nanoscience and Nanotechnology in Drug Delivery*, 257–295. https://doi.org/10.1016/B978-0-12-814029-1.00010-7

Chait, A., & den Hartigh, L. J. (2020). Adipose Tissue Distribution, Inflammation and Its Metabolic Consequences, Including Diabetes and Cardiovascular Disease. *Frontiers in Cardiovascular Medicine*, *7*, 22. https://doi.org/10.3389/FCVM.2020.00022/BIBTEX

Chen, H., Ng, J. P. M., Bishop, D. P., Milthorpe, B. K., & Valenzuela, S. M. (2018). Gold nanoparticles as cell regulators: Beneficial effects of gold nanoparticles on the metabolic profile of mice with pre-existing obesity 11 Medical and Health Sciences 1103 Clinical Sciences. *Journal of Nanobiotechnology*, *16*(1), 1–13. https://doi.org/10.1186/S12951-018-0414-6/FIGURES/3

Chen, H., Ng, J. P. M., Tan, Y., McGrath, K., Bishop, D. P., Oliver, B., Chan, Y. L., Cortie, M. B., Milthorpe, B. K., & Valenzuela, S. M. (2018). Gold nanoparticles improve metabolic profile of mice fed a high-fat diet. *Journal of Nanobiotechnology*, *16*(1). https://doi.org/10.1186/S12951-018-0338-1

Chen, Y. J., Mersmann, H. J., & Ding, S. T. (2014). Adipose Tissue Development. *Encyclopedia of Meat Sciences*, 43–48. https://doi.org/10.1016/B978-0-12-384731-7.00012-X

Chithrani, B. D., Ghazani, A. A., & Chan, W. C. W. (2006). Determining the size and shape dependence of gold nanoparticle uptake into mammalian cells. *Nano Letters*, *6*(4), 662–668. https://doi.org/10.1021/NL052396O/SUPPL_FILE/NL052396OSI20060224_104311.PDF

Connor, E. E., Mwamuka, J., Gole, A., Murphy, C. J., & Wyatt, M. D. (2005). Gold nanoparticles are taken up by human cells but do not cause acute cytotoxicity. *Small (Weinheim an Der Bergstrasse, Germany)*, *1*(3), 325–327. https://doi.org/10.1002/SMLL.200400093

Crossan, K., & Sheer, A. J. (2022). Surgical Options In the Treatment of Severe Obesity. *StatPearls*. https://www.ncbi.nlm.nih.gov/books/NBK576372/

Deng, K., Ren, C., Liu, Z., Gao, X., Fan, Y., Zhang, G., Zhang, Y., Ei-Samahy, M. A., Wang, F., & You, P. (2018). Characterization of RUNX1T1, an Adipogenesis Regulator in Ovine Preadipocyte Differentiation. *International Journal of Molecular Sciences*, *19*(5). https://doi.org/10.3390/IJMS19051300

Di Cesare, M., Sorić, M., Bovet, P., Miranda, J. J., Bhutta, Z., Stevens, G. A., Laxmaiah, A., Kengne, A. P., & Bentham, J. (2019). The epidemiological burden of obesity in childhood: A worldwide epidemic requiring urgent action. *BMC Medicine*, *17*(1), 1–20. https://doi.org/10.1186/S12916-019-1449-8/FIGURES/11

Dludla, P. V., Jack, B., Viraragavan, A., Pheiffer, C., Johnson, R., Louw, J., & Muller, C. J. F. (2018). A dose-dependent effect of dimethyl sulfoxide on lipid content, cell viability and oxidative stress in 3T3-L1 adipocytes. *Toxicology Reports*, *5*, 1014–1020. https://doi.org/10.1016/J.TOXREP.2018.10.002

Dufau, J. emy, Shen, J. X., Couchet, M., de Castro Barbosa, T., Mejhert, N., Massier, L., Griseti, E., Mouisel, E., Amri, E. Z., Lauschke, V. M., Ryden, M., & Langin, D. (2021). In vitro and ex vivo models of adipocytes. *American Journal of Physiology - Cell Physiology*, *320*(5), C822–C841. https://doi.org/10.1152/AJPCELL.00519.2020/ASSET/IMAGES/LARGE/AJPCELL.00519.2020_F004.JPEG

Eckel, J. (2018). Adipose Tissue. *The Cellular Secretome and Organ Crosstalk*, 9–63. https://doi.org/10.1016/B978-0-12-809518-8.00002-7

Elbagory, A. M., Hussein, A. A., & Meyer, M. (2019). The In Vitro Immunomodulatory Effects Of Gold Nanoparticles Synthesized From Hypoxis hemerocallidea Aqueous Extract And Hypoxoside On Macrophage And Natural Killer Cells. *International Journal of Nanomedicine*, *14*, 9007. https://doi.org/10.2147/IJN.S216972

Farmer, S. R. (2006). Transcriptional control of adipocyte formation. *Cell Metabolism*, *4*(4), 263. https://doi.org/10.1016/J.CMET.2006.07.001

Feng, X., Ding, Y., Zhou, M., Song, N., & Ding, Y. (2022). Integrative Analysis of Exosomal miR-452 and miR-4713 Downregulating NPY1R for the Prevention of Childhood Obesity. *Disease Markers*, *2022*. https://doi.org/10.1155/2022/2843353

Fruh, S. M. (2017). Obesity: Risk factors, complications, and strategies for sustainable long-term weight management. *Journal of the American Association of Nurse Practitioners*, *29*(Suppl 1), S3. https://doi.org/10.1002/2327-6924.12510

Gadde, K. M., Martin, C. K., Berthoud, H. R., & Heymsfield, S. B. (2018). Obesity: Pathophysiology and Management. *Journal of the American College of Cardiology*, *71*(1), 69–84. https://doi.org/10.1016/J.JACC.2017.11.011

Gao, L., Hu, Y., Hu, D., Li, Y., Yang, S., Dong, X., Alharbi, S. A., & Liu, H. (2020). Anti-obesity activity of gold nanoparticles synthesized from Salacia chinensis modulates the biochemical alterations in high-fat diet-induced obese rat model via AMPK signaling pathway. *Arabian Journal of Chemistry*, *13*(8), 6589–6597. https://doi.org/10.1016/J.ARABJC.2020.06.015

Gavas, S., Quazi, S., & Karpiński, T. M. (2021). Nanoparticles for Cancer Therapy: Current Progress and Challenges. *Nanoscale Research Letters*, *16*(1), 173. https://doi.org/10.1186/S11671-021-03628-6

Gavin, K. M. (2019). Origins of adult adipose progenitors. *Encyclopedia of Tissue Engineering and Regenerative Medicine*, *1–3*, 299–312. https://doi.org/10.1016/B978-0-12-801238-3.65468-5

Gregg, E. W., & Shaw, J. E. (2017). Global Health Effects of Overweight and Obesity. *New England Journal of Medicine*, *377*(1), 80–81. https://doi.org/10.1056/NEJME1706095/SUPPL_FILE/NEJME1706095_DISCLOSURES.PDF

Gregoire, F. M., Smas, C. M., & Sul, H. S. (1998). Understanding adipocyte differentiation. *Physiological Reviews*, *78*(3), 783–809. https://doi.org/10.1152/PHYSREV.1998.78.3.783/ASSET/IMAGES/LARGE/JNP.JY09F1.JPEG

Haeusler, R. A., Camastra, S., Nannipieri, M., Astiarraga, B., Castro-Perez, J., Xie, D., Wang, L., Chakravarthy, M., & Ferrannini, E. (2016). Increased bile acid synthesis and impaired bile acid transport in human obesity. *Journal of Clinical Endocrinology and Metabolism*,

101(5), 1935–1944. https://doi.org/10.1210/JC.2015-2583/SUPPL_FILE/JC-15-2583.PDF

Haiss, W., Thanh, N. T. K., Aveyard, J., & Fernig, D. G. (2007). Determination of size and concentration of gold nanoparticles from UV-vis spectra. *Analytical Chemistry*, *79*(11), 4215–4221. https://doi.org/10.1021/AC0702084

Han, H. S., & Choi, K. Y. (2021). Advances in Nanomaterial-Mediated Photothermal Cancer Therapies: Toward Clinical Applications. *Biomedicines*, *9*(3). https://doi.org/10.3390/BIOMEDICINES9030305

Hidayat, K., Du, X., & Shi, B. M. (2018). Body fatness at a young age and risks of eight types of cancer: systematic review and meta-analysis of observational studies. *Obesity Reviews*, *19*(10), 1385–1394. https://doi.org/10.1111/OBR.12705

Ho Lee, J., Seon Jeong, H., Hyun Lee, D., Beack, S., Kim, T., Lee, G.-H., Chan Park, W., Kim, C., Su Kim, K., & Kwang Hahn, S. (2017). *Targeted Hyaluronate−Hollow Gold Nanosphere Conjugate for Anti-Obesity Photothermal Lipolysis*. https://doi.org/10.1021/acsbiomaterials.7b00549

Hofmann-Amtenbrink, M., Hofmann, H., Hool, A., & Roubert, F. (2014). Nanotechnology in medicine: European research and its implications. *Swiss Medical Weekly*, *144*. https://doi.org/10.4414/SMW.2014.14044

Hossen, M. N., Kajimoto, K., Akita, H., Hyodo, M., & Harashima, H. (2012). Vascular-targeted nanotherapy for obesity: Unexpected passive targeting mechanism to obese fat for the enhancement of active drug delivery. *Journal of Controlled Release*, *163*(2), 101–110. https://doi.org/10.1016/j.jconrel.2012.09.002

Jafari, M., & Hasanzadeh, M. (2020). Cell-specific frequency as a new hallmark to early detection of cancer and efficient therapy: Recording of cancer voice as a new horizon. *Biomedicine & Pharmacotherapy*, *122*, 109770. https://doi.org/10.1016/J.BIOPHA.2019.109770

Jensen-Urstad, A. P. L., & Semenkovich, C. F. (2012). Fatty acid synthase and liver triglyceride metabolism: housekeeper or messenger? *Biochimica et Biophysica Acta*, *1821*(5), 747. https://doi.org/10.1016/J.BBALIP.2011.09.017

Jensen, C. H., Kosmina, R., Rydén, M., Baun, C., Hvidsten, S., Andersen, M. S., Christensen, L. L., Gastaldelli, A., Marraccini, P., Arner, P., Jørgensen, C. D., Laborda, J., Holst, J. J., & Andersen, D. C. (2019). The imprinted gene Delta like non-canonical notch ligand 1 (Dlk1) associates with obesity and triggers insulin resistance through inhibition of skeletal muscle glucose uptake. *EBioMedicine*, *46*, 368. https://doi.org/10.1016/J.EBIOM.2019.07.070

Jo, J., Gavrilova, O., Pack, S., Jou, W., Mullen, S., Sumner, A. E., Cushman, S. W., & Periwal, V. (2009). Hypertrophy and/or Hyperplasia: Dynamics of Adipose Tissue Growth. *PLoS*

Computational Biology, *5*(3), 1000324. https://doi.org/10.1371/JOURNAL.PCBI.1000324

Kawasaki, M., Arata, N., Miyazaki, C., Mori, R., Kikuchi, T., Ogawa, Y., & Ota, E. (2018). Obesity and abnormal glucose tolerance in offspring of diabetic mothers: A systematic review and meta-analysis. *PLOS ONE*, *13*(1), e0190676. https://doi.org/10.1371/JOURNAL.PONE.0190676

Kelly, T., Yang, W., Chen, C. S., Reynolds, K., & He, J. (2008). Global burden of obesity in 2005 and projections to 2030. *International Journal of Obesity (2005)*, *32*(9), 1431–1437. https://doi.org/10.1038/IJO.2008.102

Kershaw, E. E., & Flier, J. S. (2004). Adipose Tissue as an Endocrine Organ. *The Journal of Clinical Endocrinology & Metabolism*, *89*(6), 2548–2556. https://doi.org/10.1210/JC.2004-0395

Khan, I., Saeed, K., & Khan, I. (2019). Nanoparticles: Properties, applications and toxicities. *Arabian Journal of Chemistry*, *12*(7), 908–931. https://doi.org/10.1016/J.ARABJC.2017.05.011

Kim, B. Y. S., Rutka, J. T., & Chan, W. C. W. (2010). Nanomedicine. *Https://Doi.Org/10.1056/NEJMra0912273*, *363*(25), 2434–2443. https://doi.org/10.1056/NEJMRA0912273

Kolonin, M. G., Saha, P. K., Chan, L., Pasqualini, R., & Arap, W. (2004). Reversal of obesity by targeted ablation of adipose tissue. *Nature Medicine*, *10*(6), 625–632. https://doi.org/10.1038/NM1048

Kulebyakin, K., Tyurin-Kuzmin, P., Sozaeva, L., Voloshin, N., Nikolaev, M., Chechekhin, V., Vigovskiy, M., Sysoeva, V., Korchagina, E., Naida, D., & Vorontsova, M. (2022). Dynamic Balance between PTH1R-Dependent Signal Cascades Determines Its Pro- or Anti-Osteogenic Effects on MSC. *Cells*, *11*(21). https://doi.org/10.3390/CELLS11213519/S1

Kumar, A. (2019). The impact of obesity on cardiovascular disease risk factor. *Asian Journal of Medical Sciences*, *10*(1), 1–12. https://doi.org/10.3126/AJMS.V10I1.21294

Lee, J. E., & Ge, K. (2014). Transcriptional and epigenetic regulation of PPARγ expression during adipogenesis. *Cell & Bioscience 2014 4:1*, *4*(1), 1–11. https://doi.org/10.1186/2045-3701-4-29

Li, S., Peng, J., Wang, H., Zhang, W., Brown, J. M., Zhou, Y., & Wu, Q. (2020). Hepsin enhances liver metabolism and inhibits adipocyte browning in mice. *Proceedings of the National Academy of Sciences of the United States of America*, *117*(22), 12359–12367. https://doi.org/10.1073/PNAS.1918445117/SUPPL_FILE/PNAS.1918445117.SAPP.PDF

Li, W., Wan, H., Yan, S., Yan, Z., Chen, Y., Guo, P., Ramesh, T., Cui, Y., & Ning, L. (2020).

Gold nanoparticles synthesized with Poria cocos modulates the anti-obesity parameters in high-fat diet and streptozotocin induced obese diabetes rat model. *Arabian Journal of Chemistry*, *13*(7), 5966–5977. https://doi.org/10.1016/J.ARABJC.2020.04.031

Longo, M., Zatterale, F., Naderi, J., Parrillo, L., Formisano, P., Raciti, G. A., Beguinot, F., & Miele, C. (2019). Adipose Tissue Dysfunction as Determinant of Obesity-Associated Metabolic Complications. *International Journal of Molecular Sciences*, *20*(9). https://doi.org/10.3390/IJMS20092358

MacDougald, O. A., & Lane, M. D. (1995). Transcriptional regulation of gene expression during adipocyte differentiation. *Annual Review of Biochemistry*, *64*, 345–373. https://doi.org/10.1146/ANNUREV.BI.64.070195.002021

Manca, R., Bombillar, F., Glomski, C., & Pica, A. (2022). Obesity and immune system impairment: A global problem during the COVID-19 pandemic. *International Journal of Risk & Safety in Medicine*, *33*(2), 193–208. https://doi.org/10.3233/JRS-227007

Maples, J. M., Brault, J. J., Witczak, C. A., Park, S., Hubal, M. J., Weber, T. M., Houmard, J. A., & Shewchuk, B. M. (2015). Differential epigenetic and transcriptional response of the skeletal muscle carnitine palmitoyltransferase 1B (CPT1B) gene to lipid exposure with obesity. *American Journal of Physiology - Endocrinology and Metabolism*, *309*(4), E345–E356. https://doi.org/10.1152/AJPENDO.00505.2014

Mercer, T., Chang, A. C., Fischer, L., Gardner, A., Kerubo, I., Tran, D. N., Laktabai, J., & Pastakia, S. (2019). Mitigating The Burden Of Diabetes In Sub-Saharan Africa Through An Integrated Diagonal Health Systems Approach. *Diabetes, Metabolic Syndrome and Obesity: Targets and Therapy*, *12*, 2261. https://doi.org/10.2147/DMSO.S207427

Moore, T. L., Rodriguez-Lorenzo, L., Hirsch, V., Balog, S., Urban, D., Jud, C., Rothen-Rutishauser, B., Lattuada, M., & Petri-Fink, A. (2015). Nanoparticle colloidal stability in cell culture media and impact on cellular interactions †. *Chem. Soc. Rev*, *44*, 6287. https://doi.org/10.1039/c4cs00487f

Murphy, C. S., Liaw, L., & Reagan, M. R. (2019). In vitro tissue-engineered adipose constructs for modeling disease. *BMC Biomedical Engineering*, *1*(1). https://doi.org/10.1186/S42490-019-0027-7

Nanocomposix. (2012). Zeta Potential Analysis of Nanoparticles. *NanoComposix*, *11*, 1–6.

O'hara, S. E., Gembus, K. M., & Nicholas, L. M. (2021). Understanding the Long-Lasting Effects of Fetal Nutrient Restriction versus Exposure to an Obesogenic Diet on Islet-Cell Mass and Function. *Metabolites*, *11*(8). https://doi.org/10.3390/METABO11080514

Ou, J., Zhou, Z., Chen, Z., & Tan, H. (2019). Optical Diagnostic Based on Functionalized Gold Nanoparticles. *International Journal of Molecular Sciences 2019, Vol. 20, Page 4346*, *20*(18), 4346. https://doi.org/10.3390/IJMS20184346

Pant, R., Firmal, P., Shah, V. K., Alam, A., & Chattopadhyay, S. (2020). Epigenetic Regulation of Adipogenesis in Development of Metabolic Syndrome. *Frontiers in Cell and Developmental Biology*, *8*. https://doi.org/10.3389/FCELL.2020.619888

Patra, H. K., Banerjee, S., Chaudhuri, U., Lahiri, P., & Dasgupta, A. K. (2007). Cell selective response to gold nanoparticles. *Nanomedicine: Nanotechnology, Biology, and Medicine*, *3*(2), 111–119. https://doi.org/10.1016/J.NANO.2007.03.005

Phan, H. T., & Haes, A. J. (2019). What Does Nanoparticle Stability Mean? *The Journal of Physical Chemistry. C, Nanomaterials and Interfaces*, *123*(27), 16495. https://doi.org/10.1021/ACS.JPCC.9B00913

Pheiffer, C., Wyk, V. P. Van, Turawa, E., Levitt, N., Kengne, A. P., & Bradshaw, D. (2021). Prevalence of type 2 diabetes in South Africa: A systematic review and meta-analysis. *International Journal of Environmental Research and Public Health*, *18*(11). https://doi.org/10.3390/IJERPH18115868/S1

Phui, J., & Ng, M. (2016). *Gold nanoparticles to ameliorate obesity related glucose intolerance*. https://opus.lib.uts.edu.au/handle/10453/116906

Pike, J., & Grosse, S. D. (2018). Friction Cost Estimates of Productivity Costs in Cost-of-Illness Studies in Comparison with Human Capital Estimates: A Review. *Applied Health Economics and Health Policy*, *16*(6), 765–778. https://doi.org/10.1007/S40258-018-0416-4/TABLES/2

Poulos, S. P., Dodson, M. V., & Hausman, G. J. (2010). Cell line models for differentiation: Preadipocytes and adipocytes. *Experimental Biology and Medicine*, *235*(10), 1185–1193. https://doi.org/10.1258/EBM.2010.010063

Ramanathan, V., & Helderman, J. H. (2001). Cyclosporine Formulations. *Current and Future Immunosuppressive Therapies Following Transplantation*, 111–121. https://doi.org/10.1007/978-94-010-1005-4_6

Richard, A. J., White, U., Elks, C. M., & Stephens, J. M. (2020). Adipose Tissue: Physiology to Metabolic Dysfunction. *Endotext*. https://www.ncbi.nlm.nih.gov/books/NBK555602/

Riley, R. S., & Day, E. S. (2017). Gold nanoparticle-mediated photothermal therapy: applications and opportunities for multimodal cancer treatment. *Wiley Interdisciplinary Reviews: Nanomedicine and Nanobiotechnology*, *9*(4). https://doi.org/10.1002/WNAN.1449

Ritter, A., Kreis, N.-N., Hoock, S. C., Solbach, C., Louwen, F., & Yuan, J. (2022). Adipose Tissue-Derived Mesenchymal Stromal/Stem Cells, Obesity and the Tumor Microenvironment of Breast Cancer. In *Cancers* (Vol. 14, Issue 16). https://doi.org/10.3390/cancers14163908

Romagnoli, E., Lubrano, C., Carnevale, V., Costantini, D., Nieddu, L., Morano, S., Migliaccio, S., Gnessi, L., & Lenzi, A. (2016). Assessment of trabecular bone score (TBS) in

overweight/obese men: effect of metabolic and anthropometric factors. *Endocrine*, *54*(2), 342–347. https://doi.org/10.1007/S12020-016-0857-1

Rosen, E. D., Hsu, C. H., Wang, X., Sakai, S., Freeman, M. W., Gonzalez, F. J., & Spiegelman, B. M. (2002). C/EBPα induces adipogenesis through PPARγ: a unified pathway. *Genes & Development*, *16*(1), 22. https://doi.org/10.1101/GAD.948702

Ruiz-Ojeda, F. J., Rupérez, A. I., Gomez-Llorente, C., Gil, A., & Aguilera, C. M. (2016). Cell models and their application for studying adipogenic differentiation in relation to obesity: A review. *International Journal of Molecular Sciences*, *17*(7). https://doi.org/10.3390/IJMS17071040

Sarjeant, K., & Stephens, J. M. (2012). Adipogenesis. *Cold Spring Harbor Perspectives in Biology*, *4*(9). https://doi.org/10.1101/CSHPERSPECT.A008417

Sasidharan, A., & Monteiro-Riviere, N. A. (2015). Biomedical applications of gold nanomaterials: Opportunities and challenges. *Wiley Interdisciplinary Reviews: Nanomedicine and Nanobiotechnology*, *7*(6), 779–796. https://doi.org/10.1002/WNAN.1341

Sekar, V., Al-Ansari, M. M., Narenkumar, J., Al-Humaid, L., Arunkumar, P., & Santhanam, A. (2022). Synthesis of gold nanoparticles (AuNPs) with improved anti-diabetic, antioxidant and anti-microbial activity from Physalis minima. *Journal of King Saud University - Science*, *34*(6), 102197. https://doi.org/10.1016/J.JKSUS.2022.102197

Shan, X., Gong, X., Li, J., Wen, J., Li, Y., & Zhang, Z. (2022). Current approaches of nanomedicines in the market and various stage of clinical translation. *Acta Pharmaceutica Sinica B*, *12*(7), 3028–3048. https://doi.org/10.1016/J.APSB.2022.02.025

Sharma, N., Bhatt, G., & Kothiyal, P. (2015). Gold Nanoparticles synthesis, properties, and forthcoming applications : A review. *Indian Journal of Pharmaceutical and Biological Research*, *3*(02), 13–27. https://doi.org/10.30750/IJPBR.3.2.3

Shittu, K. O., Bankole, M. T., Abdulkareem, A. S., Abubakre, O. K., & Ubaka, A. U. (2017). Application of gold nanoparticles for improved drug efficiency. *Adv Nat Sci Nanosci Nanotechnol*, *8*(3). https://doi.org/10.1088/2043-6254/aa7716

Shukla, R., Bansal, V., Chaudhary, M., Basu, A., Bhonde, R. R., & Sastry, M. (2005). Biocompatibility of gold nanoparticles and their endocytotic fate inside the cellular compartment: A microscopic overview. *Langmuir*, *21*(23), 10644–10654. https://doi.org/10.1021/LA0513712

Sibuyi, N. R. S., Meyer, M., Onani, M. O., Skepu, A., & Madiehe, A. M. (2018). Vascular targeted nanotherapeutic approach for obesity treatment. *International Journal of Nanomedicine*, *13*, 7915. https://doi.org/10.2147/IJN.S173424

Sibuyi, N. R. S., Moabelo, K. L., Fadaka, A. O., Meyer, S., Onani, M. O., Madiehe, A. M., & Meyer, M. (2021). Multifunctional Gold Nanoparticles for Improved Diagnostic and

Therapeutic Applications: A Review. *Nanoscale Research Letters*, *16*(1). https://doi.org/10.1186/S11671-021-03632-W

Nanotechnology advances towards development of targeted-treatment for obesity, 17 Journal of Nanobiotechnology 122 (2019). https://doi.org/10.1186/s12951-019-0554-3

Sibuyi, N. R. S., Moabelo, K. L., Meyer, M., Onani, M. O., Dube, A., & Madiehe, A. M. (2019). Nanotechnology advances towards development of targeted-treatment for obesity. *Journal of Nanobiotechnology*, *17*(1), 1–21. https://doi.org/10.1186/s12951-019-0554-3

Sibuyi, N. R. S., Moabelo, K. L., Meyer, S., Skepu, A., Onani, M. O., Madiehe, A. M., & Meyer, M. (2022). Nanotechnology-Based Strategies for Treatment of Obesity, Cancer and Anti-microbial Resistance: Highlights of the Department of Science and Innovation/Mintek Nanotechnology Innovation Centre Biolabels Research Node at the University of the Western Cape. *Applied Sciences*, *12*(20), 10512. https://doi.org/10.3390/APP122010512

Sibuyi, N. R., Thovhogi, N., Gabuza, K. B., Meyer, M. D., Drah, M., Onani, M. O., Skepu, A., Madiehe, A. M., & Meyer, M. (2017). Peptide-functionalized nanoparticles for the selective induction of apoptosis in target cells. *Https://Doi.Org/10.2217/Nnm-2017-0085*, *12*(14), 1631–1645. https://doi.org/10.2217/NNM-2017-0085

Simu, S. Y., Ahn, S., Castro-Aceituno, V., Singh, P., Mathiyalagan, R., Jiménez-Pérez, Z. E., Hurh, J., Oi, L. Z., Hun, N. J., Kim, Y.-J., & Yang, D.-C. (2018). Gold Nanoparticles Synthesized with Fresh Panax ginseng Leaf Extract Suppress Adipogenesis by Downregulating PPAR γ /CEBP α Signaling in 3T3-L1 Mature Adipocytes . *Journal of Nanoscience and Nanotechnology*, *19*(2), 701–708. https://doi.org/10.1166/JNN.2019.15753

Sirajudeen, S., Shah, I., & Al Menhali, A. (2019). A Narrative Role of Vitamin D and Its Receptor: With Current Evidence on the Gastric Tissues. *International Journal of Molecular Sciences*, *20*(15). https://doi.org/10.3390/IJMS20153832

Smith, J. D., Fu, E., & Kobayashi, M. A. (2020). Prevention and Management of Childhood Obesity and its Psychological and Health Comorbidities. *Annual Review of Clinical Psychology*, *16*, 351. https://doi.org/10.1146/ANNUREV-CLINPSY-100219-060201

Sosibo, N. M., Keter, F. K., Skepu, A., Tshikhudo, R. T., Revaprasadu, N., & Sosibo, N. M. (2015). Facile Attachment of TAT Peptide on Gold Monolayer Protected Clusters: Synthesis and Characterization. *Nanomaterials (Basel, Switzerland)*, *5*(3), 1211–1222. https://doi.org/10.3390/NANO5031211

Sousa De Almeida, M., Susnik, E., Drasler, B., Taladriz-Blanco, P., Petri-Fink, A., & Rothen-Rutishauser, B. (2021). Understanding nanoparticle endocytosis to improve targeting strategies in nanomedicine. *Chemical Society Reviews*, *50*(9), 5397. https://doi.org/10.1039/D0CS01127D

Stienstra, R., Duval, C., Müller, M., & Kersten, S. (2007). PPARs, Obesity, and Inflammation. *PPAR Research*, *2007*. https://doi.org/10.1155/2007/95974

Sugiyama, M., Kikuchi, A., Misu, H., Igawa, H., Ashihara, M., Kushima, Y., Honda, K., Suzuki, Y., Kawabe, Y., Kaneko, S., & Takamura, T. (2018). Inhibin βE (INHBE) is a possible insulin resistance-associated hepatokine identified by comprehensive gene expression analysis in human liver biopsy samples. *PLOS ONE*, *13*(3), e0194798. https://doi.org/10.1371/JOURNAL.PONE.0194798

Sun, S., Cao, X., Castro, L. F. C., Monroig, Ó., & Gao, J. (2021). A network-based approach to identify protein kinases critical for regulating srebf1 in lipid deposition causing obesity. *Functional and Integrative Genomics*, *21*(5–6), 557–570. https://doi.org/10.1007/S10142-021-00798-5/FIGURES/7

Sung, J. H., Chon, J. W., Lee, M. A., Park, J. K., Woo, J. T., & Park, Y. K. (2011). The anti-obesity effect of Lethariella cladonioides in 3T3-L1 cells and obese mice. *Nutrition Research and Practice*, *5*(6), 503–510. https://doi.org/10.4162/NRP.2011.5.6.503

Szklarczyk, D., Kirsch, R., Koutrouli, M., Nastou, K., Mehryary, F., Hachilif, R., Gable, A. L., Fang, T., Doncheva, N. T., Pyysalo, S., Bork, P., Jensen, L. J., & von Mering, C. (2023). The STRING database in 2023: protein-protein association networks and functional enrichment analyses for any sequenced genome of interest. *Nucleic Acids Research*, *51*(D1), D638–D646. https://doi.org/10.1093/NAR/GKAC1000

Tak, Y. J., & Lee, S. Y. (2021). Anti-Obesity Drugs: Long-Term Efficacy and Safety: An Updated Review. *The World Journal of Men's Health*, *39*(2). https://doi.org/10.5534/WJMH.200010

Thovhogi, N., Sibuyi, N., Meyer, M., Onani, M., & Madiehe, A. (2015). Targeted delivery using peptide-functionalised gold nanoparticles to white adipose tissues of obese rats. *Journal of Nanoparticle Research*, *17*(2). https://doi.org/10.1007/S11051-015-2904-X

Thovhogi, N., Sibuyi, N. R. S., Onani, M. O., Meyer, M., & Madiehe, A. M. (2018a). Peptide-functionalized quantum dots for potential applications in the imaging and treatment of obesity. *International Journal of Nanomedicine*, *13*, 2551–2559. https://doi.org/10.2147/IJN.S158687

Thovhogi, N., Sibuyi, N. R. S., Onani, M. O., Meyer, M., & Madiehe, A. M. (2018b). Peptide-functionalized quantum dots for potential applications in the imaging and treatment of obesity. *International Journal of Nanomedicine*, *13*, 2551. https://doi.org/10.2147/IJN.S158687

Todorčević, M., Hilton, C., McNeil, C., Christodoulides, C., Hodson, L., Karpe, F., & Pinnick, K. E. (2017). A cellular model for the investigation of depot specific human adipocyte biology. *Adipocyte*, *6*(1), 40–55. https://doi.org/10.1080/21623945.2016.1277052

Toriola, A. L., Moselakgomo, V. K., Shaw, B. S., & Goon, D. T. (2016). Overweight, obesity

and underweight in rural black South African children. *Http://Dx.Doi.Org/10.1080/16070658.2012.11734406*, *25*(2), 57–61. https://doi.org/10.1080/16070658.2012.11734406

Umer, A., Kelley, G. A., Cottrell, L. E., Giacobbi, P., Innes, K. E., & Lilly, C. L. (2017). Childhood obesity and adult cardiovascular disease risk factors: A systematic review with meta-analysis. *BMC Public Health*, *17*(1), 1–24. https://doi.org/10.1186/S12889-017-4691-Z/FIGURES/14

Velazquez, A., & Apovian, C. M. (2018). Updates on obesity pharmacotherapy. *Annals of the New York Academy of Sciences*, *1441*(1), 106–119. https://doi.org/10.1111/nyas.13542

Villiers, C. L., Freitas, H., Couderc, R., Villiers, M. B., & Marche, P. N. (2010). Analysis of the toxicity of gold nano particles on the immune system: effect on dendritic cell functions. *Journal of Nanoparticle Research*, *12*(1), 55. https://doi.org/10.1007/S11051-009-9692-0

Wang, X., Yang, T., Yu, Z., Liu, T., Jin, R., Weng, L., Bai, Y., Gooding, J. J., Zhang, Y., & Chen, X. (2022). Intelligent Gold Nanoparticles with Oncogenic MicroRNA-Dependent Activities to Manipulate Tumorigenic Environments for Synergistic Tumor Therapy. *Advanced Materials*, *34*(15), 2110219. https://doi.org/10.1002/ADMA.202110219

WHO. (2008). *Waist Circumference and Waist-Hip Ratio: Report of a WHO Expert Consultation*. www.who.int

WHO. (2020). *Obesity and overweight*. https://www.who.int/news-room/fact-sheets/detail/obesity-and-overweight

WHO. (2022). Global Health Observatory. *WHO*.

Wu, F. Y., & Yin, R. X. (2022). Recent progress in epigenetics of obesity. *Diabetology & Metabolic Syndrome 2022 14:1*, *14*(1), 1–30. https://doi.org/10.1186/S13098-022-00947-1

Wu, Z., & Wang, S. (2013). Role of kruppel-like transcription factors in adipogenesis. *Developmental Biology*, *373*(2), 235–243. https://doi.org/10.1016/J.YDBIO.2012.10.031

Wusu, A. D., Remaliah, N., Sibuyi, S., Moabelo, K. L., Goboza, M., Madiehe, A., & Meyer, M. (2022). Citrate-capped gold nanoparticles with a diameter of 14 nm alter the expression of genes associated with stress response, cytoprotection and lipid metabolism in CaCo-2 cells. *Nanotechnology*, *33*, 105101–105112. https://doi.org/10.1088/1361-6528/ac3c7c

Xia, Q., Huang, J., Feng, Q., Chen, X., Liu, X., Li, X., Zhang, T., Xiao, S., Li, H., Zhong, Z., & Xiao, K. (2019). Size- and cell type-dependent cellular uptake, cytotoxicity and in vivo distribution of gold nanoparticles. *International Journal of Nanomedicine*, *14*, 6957. https://doi.org/10.2147/IJN.S214008

Xie, X., Liao, J., Shao, X., Li, Q., & Lin, Y. (2017). The Effect of shape on Cellular Uptake of

Gold Nanoparticles in the forms of Stars, Rods, and Triangles. *Scientific Reports*, *7*(1). https://doi.org/10.1038/S41598-017-04229-Z

Yadav, H. M., & Jawahar, A. (2022). Environmental Factors and Obesity. *StatPearls*. https://www.ncbi.nlm.nih.gov/books/NBK580543/

Yeh, Y. C., Creran, B., & Rotello, V. M. (2012). Gold Nanoparticles: Preparation, Properties, and Applications in Bionanotechnology. *Nanoscale*, *4*(6), 1871. https://doi.org/10.1039/C1NR11188D

Yi, M. H., Simu, S. Y., Ahn, S., Aceituno, V. C., Wang, C., Mathiyalagan, R., Hurh, J., Batjikh, I., Ali, H., Kim, Y.-J., Kim, S., & Yang, D.-C. (2020). Anti-obesity Effect of Gold Nanoparticles from Dendropanax morbifera Léveille by Suppression of Triglyceride Synthesis and Downregulation of PPARγ and CEBPα Signaling Pathways in 3T3-L1 Mature Adipocytes and HepG2 Cells . *Current Nanoscience*, *16*(2), 196–203. https://doi.org/10.2174/1573413716666200116124822

Zheng, X., Zhang, P., Fu, Z., Meng, S., Dai, L., & Yang, H. (2021). Applications of nanomaterials in tissue engineering. *RSC Advances*, *11*(31), 19041–19058. https://doi.org/10.1039/D1RA01849C